

1-1-2006

Dynamic property characterization of ionic polymer metal composite (Ipmc)

Prashanth Reddy Duvvuru Kamakshi
University of Nevada, Las Vegas

Follow this and additional works at: <https://digitalscholarship.unlv.edu/rtds>

Repository Citation

Duvvuru Kamakshi, Prashanth Reddy, "Dynamic property characterization of ionic polymer metal composite (Ipmc)" (2006). *UNLV Retrospective Theses & Dissertations*. 1949.
<http://dx.doi.org/10.25669/62jo-w362>

This Thesis is protected by copyright and/or related rights. It has been brought to you by Digital Scholarship@UNLV with permission from the rights-holder(s). You are free to use this Thesis in any way that is permitted by the copyright and related rights legislation that applies to your use. For other uses you need to obtain permission from the rights-holder(s) directly, unless additional rights are indicated by a Creative Commons license in the record and/or on the work itself.

This Thesis has been accepted for inclusion in UNLV Retrospective Theses & Dissertations by an authorized administrator of Digital Scholarship@UNLV. For more information, please contact digitalscholarship@unlv.edu.

DYNAMIC PROPERTY CHARACTERIZATION OF IONIC POLYMER METAL
COMPOSITE (IPMC)

by

Prashanth Reddy Duvvuru Kamakshi

Bachelor of Science in Mechanical Engineering
Madras University, India
April 2003

A thesis submitted in partial fulfillment
of the requirements for the

Master of Science Degree in Engineering
Department of Mechanical Engineering
Howard R. Hughes College of Engineering

Graduate College
University of Nevada, Las Vegas
May 2006

UMI Number: 1436762

INFORMATION TO USERS

The quality of this reproduction is dependent upon the quality of the copy submitted. Broken or indistinct print, colored or poor quality illustrations and photographs, print bleed-through, substandard margins, and improper alignment can adversely affect reproduction.

In the unlikely event that the author did not send a complete manuscript and there are missing pages, these will be noted. Also, if unauthorized copyright material had to be removed, a note will indicate the deletion.

UMI[®]

UMI Microform 1436762

Copyright 2006 by ProQuest Information and Learning Company.

All rights reserved. This microform edition is protected against unauthorized copying under Title 17, United States Code.

ProQuest Information and Learning Company
300 North Zeeb Road
P.O. Box 1346
Ann Arbor, MI 48106-1346



Thesis Approval
The Graduate College
University of Nevada, Las Vegas

January 20, 2006

The Thesis prepared by

Prashanth Reddy Duvvuru Kamakshi

Entitled

Dynamic Property Characterization of Ionic Polymer Metal Composite

(IPMC)

is approved in partial fulfillment of the requirements for the degree of

Master of Science Mechanical Engineering

A handwritten signature in black ink, appearing to read "Alpin", written over a horizontal line.

Examination Committee Chair

A handwritten signature in black ink, appearing to read "Dale Shultz", written over a horizontal line.

Dean of the Graduate College

A handwritten signature in black ink, appearing to read "Ajay K. Roy", written over a horizontal line.

Examination Committee Member

A handwritten signature in black ink, appearing to read "M.B. Taha", written over a horizontal line.

Examination Committee Member

A handwritten signature in black ink, appearing to read "S. S. S.", written over a horizontal line.

Graduate College Faculty Representative

ABSTRACT

Dynamic Property Characterization of Ionic Polymer Metal Composite (IPMC)

by

Prashanth Reddy Duvvuru Kamakshi

Dr. Woosoon Yim, Examination Committee Chair
Professor of Mechanical Engineering
University of Nevada, Las Vegas

In this thesis dynamic properties of Ionic Polymer Metal Composite (IPMC) is studied. The ionic polymer (IPMC) is made out of a high polymer gel film whose surface is plated with platinum. This ionic polymer finds its application in future as artificial muscle. Analytical modeling method for both single and segmented ionic polymer which can exhibit varying curvature along the polymer was introduced. This segmented ionic polymer can generate more flexible propulsion compared with a single strip ionic polymer where only forward propulsion can be generated by a simple oscillatory bending motion. It is well known in biomimetic system research that a simple bending motion has lower efficiency than a snake –like wavy motion in propulsion. In this segmented ionic polymer each segment can be bent individually. This segmented ionic polymer design consists of a number of independent electrode sections along the length of the ionic polymer to realize the undulatory motion by selectively activating each segment. The magnitude of curvature can be controlled by adjusting the voltage level applied across each segment.

In this thesis we focus on the development of an analytical model to predict the deflection of this single and segmented ionic polymers and the model is validated with experimental results. Due to the complexity of the polymer , it is necessary to find the dynamic parameters from the experimental data. After proper tuning of dynamic model, this can be used for various control applications including the underwater robotic propulsor device design and others. The dynamic model developed in this work reasonable complies with experimental data and can be further developed for future control algorithm design.

TABLE OF CONTENTS

ABSTRACT	iii
LIST OF FIGURES	vii
ACKNOWLEDGMENTS	x
CHAPTER 1 INTRODUCTION	1
1.1 Introduction and history of modeling	1
1.2 Description	1
1.3 Characterization	2
1.4 Literature review	4
1.5 Modeling	5
1.5.1 Physical model	5
1.5.2 Black box model	6
1.5.3 Gray box model	7
1.6 Problem definition	9
1.7 Overview	10
CHAPTER 2 DYNAMIC MODELING	11
2.1 Hypotheses on motion principles	11
2.2 Analytical model	12
2.3 RC model of ionic polymer	13
2.4 Relaxation model	14
2.5 Finite element modeling of segment ionic polymer	15
2.6 State space model development	19
CHAPTER 3 EXPERIMENT SETUP	22
3.1 Experiment description	24
3.2 Control signal for ionic polymer	25
3.3 Blocking force measurement of ionic polymer	25
3.4 Deflection measurement of the ionic polymer	26
3.5 Interfacing image acquisition and dSPACE 1104	27
3.6 Image processing	29
3.6.2 Image enhancing & analysis	30
3.6.3 Binary conversion	31
3.6.4 Data approximation	32
3.7 Pre chemical processing of ionic polymer	33
3.8 Integration of vision system with dSPACE	34

CHAPTER 4 RESULTS AND DISCUSSION	39
4.1 Experimental results.....	39
4.1.1 Deflection response for 2.5 Volt step input	40
4.1.2 Deflection response of ionic polymer for 3 Volt Step Input.....	43
4.1.3 Additional observations	45
4.1.4 Blocking force response.....	46
4.1.5 Experiments conducted with segmented ionic polymer	50
4.2 Computer simulated results of segmented ionic polymer.....	53
4.3 Experimental validation of the simulation results.	55
CHAPTER 5 CONCLUSION AND FUTUREWORK	59
5.1 Conclusion	59
5.2 Recommended future work.....	60
5.2.1 Large deflection model	60
5.2.2 Segmented ionic polymer	61
5.2.3 Hydrodynamic modeling	61
5.2.4 Control	61
APPENDIX A – EXPERIMENTAL APPARATUS	62
A.1 Bi - Polar Voltage amplifier.....	62
A.2 Ionic Polymer Metallic Composite Actuator	62
A.3 Step UP/Down Transformer	63
A.4 Load Cell.....	63
A.5 Camera	63
A.6 dSPACE DS-1104 Controller board	64
A.7 Signal Conditioner	64
A.8 Rapid Prototyping Machine	65
APPENDIX B – MATLAB® CODE.....	66
B.1 image_cap_movie_generator.m	66
B.2 vol_cur.m	66
B.3 tip_deflection.m	67
B.4 Act_4volt.m	68
B.5 IPMC_tip_deflection.m	69
B.6 main.m	70
B.7 fexi.m	71
B.8 mexi.m	72
B.9 kexi.m.....	73
B.10 plt_beam.m.....	74
B.11 plt.-misc	75
B.12 sim_1.m.....	75
BIBLIOGRAPHY	76
VITA.....	78

LIST OF FIGURES

Figure 1.1	Chemical structure typical ionic polymer	2
Figure 1.2	Sample of ionic polymer	3
Figure 1.3	Actuator configuration for the Xiao and Bhattacharya (2001).....	7
Figure 1.4	RC configuration of ionic polymer	8
Figure 2.1	Ionic polymer with N segments.....	12
Figure 2.2	R-C circuit of ionic polymer	13
Figure 2.3	shows a schematic of the ionic polymer.....	16
Figure 2.4	i-th segment illustrating nodal displacement.....	17
Figure 3.1	Schematic diagram illustrating basic experimental setup	22
Figure 3.2	Actual experiment setup	23
Figure 3.3	IPMC setup with polymer holding Device.....	24
Figure 3.4	Load Cell Setup	26
Figure 3.5	Interfacing of MATLAB with Real time Processor of dSPACE	28
Figure 3.6	Tasks of image processing	29
Figure 3.7	Sample image	30
Figure 3.8	Image enhancing.....	31
Figure 3.9	Binary image	32
Figure 3.10	Camera positioning.....	35
Figure 3.11	Arrow direction indicating the y-axis increases from top to bottom.....	36
Figure 3.12	Finding the tip displacement by considering the data point with highest 'x' value	37
Figure 4.1	Ionic polymer holder	39
Figure 4.2	Current response of the ionic polymer for 2.5 V step input	41
Figure 4.3	Experiment deflection of the ionic polymer for 2.5 volts step input.....	42
Figure 4.4	Tip displacement curves of the ionic polymer for 2.5 volts	42
Figure 4.5	Current response of the ionic polymer for 3 V step input	43
Figure 4.6	Experiment deflection of the ionic polymer for 3 Volts step input.....	44
Figure 4.7	Tip displacement curves of the ionic polymer for 2.5 volts	44
Figure 4.8	Current with 2V,3V, 3.5V and 4V step inputs	45
Figure 4.9	Experimental free deflection with 2V, 3V, 3.5V, 4V	45
Figure 4.10	Blocking force for two different size of polymer with large cation	48
Figure 4.11	Blocking force polymer with small ion.....	49
Figure 4.12	Segmented ionic polymer	50
Figure 4.13	Experiment setup of Segmented ionic polymer	51
Figure 4.14	Input voltage and output response segmented ionic polymer	52
Figure 4.15	Simulated plots for 2V, 1V and -2V (n=3).....	54
Figure 4.16	Simulated plots for 2V, 1V and -2V (n=3).....	55
Figure 4.17	Experimental Vs Simulated tip Deflection for step input 2.5V	56

Figure 4.18	Experimental Vs Simulated current response	56
Figure 4.19	Simulated and Experimental Shape of ionic polymer for 2.5V step input.....	57
Figure 4.20	Experimental Vs Simulated tip deflection for step input 3V	57
Figure 4.21	Experimental Vs Simulated current response for 3 V.....	58
Figure 4.22	Simulated and Experimental shape of ionic polymer for 3V step input.....	58

ACKNOWLEDGMENTS

First, I would like to sincerely thank my advisor Dr. Woosoon Yim for his continuous support in my Masters program. He showed me different ways to approach a research project and the need to be persistent to accomplish any goal. His understanding, encouragement and personal guidance has provided a good basis for this thesis. It was a great pleasure to conduct research under his supervision.

I take this opportunity to thank Dr. Mohamed B. Trabia , Dr. Sahajendra Singh and Dr. Ajit K. Roy for serving on the committee and reviewed my work on a very short notice. Their valuable feedback helped me to improve my thesis in many ways.

I thank my parents, D.Subrahmanyam and D.Sarmista for giving me life in the first place, also for their unconditional love and encouragement to pursue my interest even when interest went beyond boundaries of language, field and geography. I solely dedicate this work to my parents

During this tenure I have worked with many colleagues for whom I have great regard and I wish to extend my warm wishes to all those who have helped me with my work in Dept of Mechanical Engineering. Especially I thank my friends Vijaysarathy, Kiran Parimi, Jamil M. Renno, Brinda Holur Venkatesh , Masoud Fegghi, Shivakanth, Venkat, Kofi Cobbinah. I enjoyed all the discussions we had on various topics and had lots of fun being in your group. I thank National Science Foundation for supporting my research program financially.

CHAPTER 1

INTRODUCTION

1.1 Introduction and history of modeling

Ionic polymer metal composite (IPMC) are a class of active material that exhibits electromechanical coupling. For convenience Ionic Polymer Metal Composite(IPMC) is referred as ionic polymer. Ionic polymer materials generally consist of a Perfluorinate membrane that has been plated on both sides with a conductive metal. Application of an electric field across the thickness of the material produces mechanical deformation. Conversely, mechanical deformation of the material produces a measurable electrical signal. Thus, ionic polymers can be used as both sensors and actuators for applications in motion measurement and control. The advantage of these materials compared to other types of actuators is that they are materials that operate in a hydrated environment. This has motivated the development of biomimetic actuators that exploit their unique properties.

1.2 Description

Ion-exchange polymer-metal composites (IPMC) are active actuators that show large deformation in the presence of low applied voltage and exhibit low impedance. They operate best in a humid environment and can be made as self-contained encapsulated actuators to operate in dry environments as well. They provide an attractive means of

actuation as artificial muscles for biomechanics and biomimetics applications. The ionic polymer muscle used in our investigation is composed of a per fluorinated ion exchange membrane (IEM), which is chemically composed with a noble metal such as gold or platinum. In our case it was Platinum. A typical chemical structure of one of the ionic polymers used in our research is shown in Figure 1.1

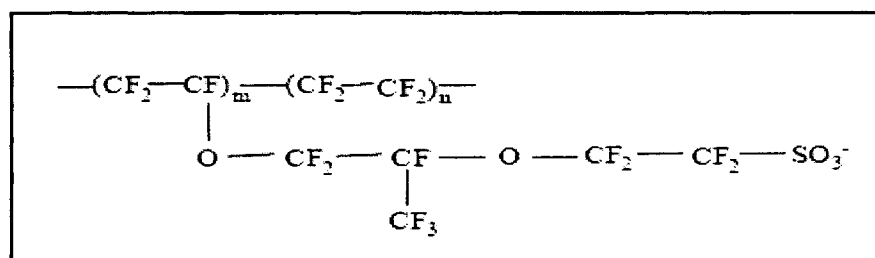


Figure 1.1 Chemical structure typical ionic polymer

Where n is such that $5 < n < 11$ and $m \sim 1$, and M^+ is the counter ion (H^+ , Li^+ or Na^+). One of the interesting properties of this material is its ability to absorb large amounts of polar solvents, i.e. water. Platinum, Pt, metal ions, which are dispersed through out the hydrophilic regions of the polymer, are subsequently reduced to the corresponding metal atoms. This results in the formation of a dendritic type electrode. The discussion of the early history of these materials and their use as biomimetic transducers is referred in [1].

1.3 Characterization

Most ionic polymer actuators experiments have been performed on samples based on DuPont's Nafion 117, a readily available commercial polymer. The overwhelming majority of experiments have been performed on actuators in a cantilevered bender

configuration. A sample of the above ionic polymer is shown Figure 1.2. Typical dimensions are 5mm wide and 10mm or more in length but it can be made in any size. They function best in the fully hydrated state and their performance as actuators decreases rapidly as they dry out. Thus ionic polymers are 'soft' and 'wet' actuators.



Figure 1.2 Sample of ionic polymer

Reported values of their modulus vary from approximately 0.1GPa [13] to over 0.6GPa [5]. Note that this modulus includes the stiffening effect of the electrode, which is significant. Since the electrode thickness and structure depend on the details of the plating process, which has not been standardized in our case it was 0.8GPa.

Although the experimental data presented by various researchers correspond to ionic polymers with different dimensions, electrode materials, neutralizing ions, etc, it is still possible to generalize the attributes of ionic polymer transducers from the collection of experimental results.

1.4 Literature review

Previous modeling efforts for ionic polymer materials can generally be separated into empirical models or models based on first principles.

Models based on first principle forms a basis for understanding the general and fundamental features. The critical parameters are defined operationally in terms of measurable fundamental parameters, so the mechanistic basis of the mode can be evaluated by testing both assumptions and prediction. To the extent that available data permit such evaluations, they generally support the model for many classes of system.

Models of electromechanical impedance were developed for the purpose of relating applied voltage to current [2]. Early work on these materials utilized a linear model of actuation to estimate the relationship between applied field and mechanical deformation [3]. Both of these models utilized curve fits of experimental data to model electromechanical coupling. Two port electromechanical model [4] that accounted for both sensing and actuation within the material. This model was also based on curve fits of experimental data. Models based on first principles have also been developed [5-9]. These models are based on the interaction of electrostatic and hydraulic forces within the polymer membrane [8-9] place more emphasis on the electrostatic interaction while the models by [6], [7], [8] are based on the relationship between solvent flux and pressure gradients of the models.

Our work complements the recent paper by [6], [11] and [12] in which the charge–deformation relationship was explored in depth for current excitation of polymer benders. Finite element approach is used to describe the dynamics of the segmented IPMC, which considered as composed of finite elements satisfying Euler-Bernoulli's beam theory.

1.5 Modeling

According to Newbury [4] most of the models proposed for ionic polymers can be placed in one of the three categories.

1. Physical model
2. Black box model
3. Gray box model

1.5.1 Physical model

The first complete physical models that were both solved and compared to experimental results were not published until, presented what they termed a 'white-box' [6,7] model for ionic polymer actuators. They proposed that the application of a step voltage (electric field) causes the mobile cations to quickly migrate across the thickness of the actuator from the anode (positive electrode) to the cathode (negative electrode), dragging water molecules along with them. The resulting change in water concentration, a decrease at the anode and an increase at the cathode, causes contraction and expansion of the respective portions of the base polymer and induces a curvature in the ionic actuator.

Central to the micromechanics model [5,9] is the idea that the side chains of the polymer form clusters, which are saturated by water when the polymer is hydrated. Under the application of an electric field, the cations are redistributed, migrating towards the cathode. A locally imbalanced net charge density results and the associated electrostatic forces produce stresses that act on the polymer backbone, resulting in an electrically induced curvature of the polymer.

The micro molecular model [5,9] of electromechanical coupling based on osmotic pressure and electrostatic forces within the polymer substrate . Comparison between

experiment and theory was provided for tip displacement with sinusoidal input voltage. While these novel smart method composites have many potential applications, the mechanisms which control their macroscopic behavior have not been fully understood. The constitute parameters in the proposed model are estimated based on the microstructure of the composite, using micromechanics, or they are determined from the experiments. Central to the theory is the recognition that the internal stresses produced by the presence of electrically unbalanced negative ions that permanently fixed to the backbone ionic polymer. Although the osmotic effects are also relevant, they have less impact in defining the initial actuation and subsequent relaxation of the Nafion based ionic polymer. The formulation presented in this paper gave detailed structure to each competing factor and suggested a path for further parametric and experimental studies.

Difficulty with physical modeling of ionic polymer transducers is that the chemical and physical mechanisms responsible for the electromechanical transduction have not been accurately identified. Also, the material parameters that appear in many of the proposed equations are not well known and do not lend themselves to direct measurement. Another issue with the physical models is that the governing equations are quite complex. These models will most likely prove useful in identifying and understanding the mechanisms responsible for transduction; however, much simpler models are needed for engineering design.

1.5.2 Black box model

According to Newbury [4] the first black box model of ionic polymer actuation was presented by [2]. They used experimental tip displacement data with voltage step inputs

in conjunction with a least squares algorithm to determine values for the constants. Another linear model of actuation to estimate the relationship between applied field and mechanical deformation was proposed [6]. In this study, the electrical characteristics of the actuator were represented by the surface resistances of the gel membrane permeated with water, and series connection of resistance and capacitance. Another black box model for cantilevered ionic polymer benders was put forth by [15]. They used the first-order differential equation

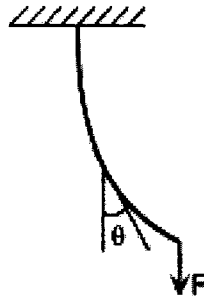


Figure 1.3. Actuator configuration for the Xiao and Bhattacharya (2001)

While the black box models are relatively easy to understand and use, their scope is limited as they cannot accommodate any changes in actuator dimensions.

1.5.3 Gray box model

The most widely accepted gray box actuator model was presented by [6]. They represented the ionic polymer using three 'stages' that were connected in series as shown in Figure 1.4, an electrical stage, a stress-generation stage, and a mechanical stage.

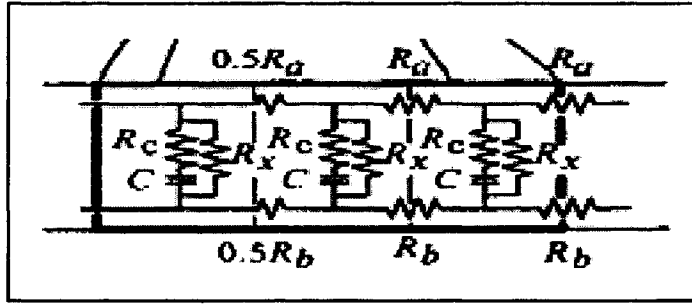


Figure 1.4 RC configuration of ionic polymer

The input of the electrical stage was the applied voltage and the output was current. This current was used as an input to the stress-generation stage. The second-order terms were used to provide dynamics in the relationship between the current and the induced stress. No proper verification of the model's scalability was presented [11].

1.6 Problem definition

Our goal is to introduce an analytical method for both single and segmented ionic polymer which can exhibit varying curvature along the polymer. This objective can be accomplished through a combination and verification of modeling and experimental work. The purpose of considering segmented ionic polymer is, simple bending motion has lower efficiency than a snake like wavy motion in propulsion which have been found by biological analysis of the swimming mechanism of fish or other creatures. To realize more complex motions, such as multi- DOF motion, segmented ionic polymer of which could be bent individually is needed. The magnitude of the curvature can be controlled by adjusting the voltage level applied across each segment.

With the fundamental material parameters determined this analytical model can help scientific and engineering communities understanding of the macroscopic behavior of ionic polymer actuators.

Most of the experimental work done until now used Laser deflection monitoring system to monitor the deflection of the ionic polymer which cannot be efficient for large deflection. So we developed the Vision system using BASLER A602f camera as an Image capturing device and developed an image processing technique for processing image data for monitoring large deflection of ionic polymer with better efficiency.

1.7 Overview

The following is a brief summary for the organization of the thesis. Chapter 2 describes dynamic modeling for the ionic polymer based on RC model and finite element method. The experimental setup used in Chapter 2 be discussed in Chapter 3 including vision system used to measure the dynamic deformation of the ionic polymer. Chapter 4 presents the computer simulation results and experiments presented for validations our modeling methods. Chapter 5 includes the conclusions of this research work and suggestions for future work.

CHAPTER 2

DYNAMIC MODELING

Ionic polymer metallic composite (IPMC) is one of the electro active polymers (EAP) that have shown potentials for many applications in robotics and other small scale system. This ionic polymer is electro active polymer (EAP) material that bends when subjected to voltage across its thickness. Ionic polymer has several attractive EAP characteristics that include:

- Low drive voltage -4.0 to 4.0 V
- Soft material ($E = 1.158 \text{ GPa}$)
- Possible to miniaturization ($< 1 \text{ mm}$)
- Can be activated in water or in wet conditions.

2.1 Hypotheses on motion principles

The following hypothesis on the motion mechanisms are introduced in this paper:

- Voltage applied on the polymer yields an electric field through the membrane.
- Nafion ions migrate from the anode to the cathode by electrostatic force.
- Hydration causes travel of water molecules with the Nafion ions.

The following forces were applied on the ionic polymer membrane by the travel of the nafion ions and the water molecules, which results in the bending of ionic polymer.

- Swell and contraction caused by the water content change.

- Momentum conservation effect concerning the ionic migration and water travel.
- Conformation change of the polymer structure according to ionic migration.

2.2 Analytical model

Analytical model was developed based on the clumped RC model [11] of the ionic polymer and beam bending theory accounting for small deflections. This dynamic model focuses on the macro models for the electric inputs and electromechanical actuation of ionic polymer. The macro model that relates the electric input and mechanical output are required for the material characterization i.e. to define and extract the parameters in order to support potential application establishing a mathematical base for actuator design.

Finite element method is used to describe the dynamics of the both single and multiple segmented ionic polymers, where each element satisfies Euler Bernoulli's beam theory. The schematic diagram of segmented ionic polymer is shown in Figure. 2.1

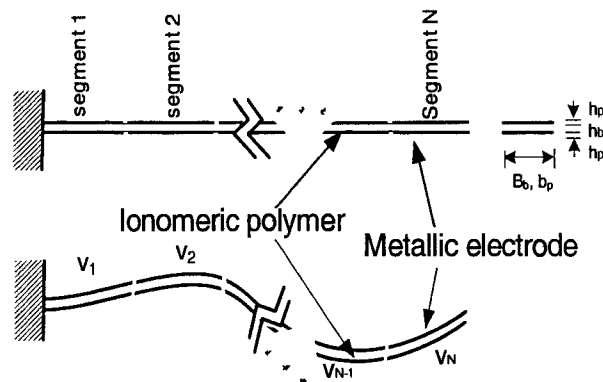


Figure 2.1 Ionic polymer with N segments

The energy approach is used to formulate the equation of motion where the bending moment applied in each element is assumed to be proportional to the bending curvature determined from the clamped RC model. The modeling steps are described in following section.

It has to be noted that from previous experiments performed [11], the clumped RC modeling hold good only for Nafion based ionic polymer strip and quite large difference between the model and the experimental results is observed for Flemion based ionic polymer.

2.3 RC model of ionic polymer

The clumped RC model relates the input voltage applied to the ionic polymer strip to the charge. The ionic polymer has two parallel electrodes and electrolyte between them. Double-layer capacitors are formed on the interfaces of two electrodes and the electrolyte. The electrolyte between the electrodes may introduce as internal resistance. This series circuit of C-R-C circuit can be simplified to R-C circuit as shown in Figure 2.2

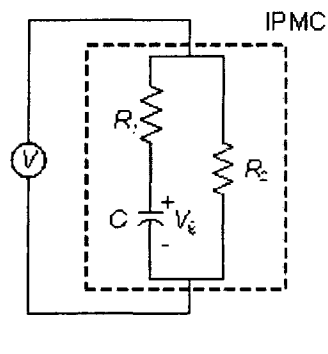


Figure 2.2 R-C circuit of ionic polymer

For a voltage input to the segment i , V_i , the electric charge, Q_i and the current, I_i , in the circuit become

$$\frac{Q_i}{V_i} = \frac{C}{R_1Cs + 1} \quad (2.1)$$

$$\frac{I_i}{V_i} = \frac{C(R_1 + R_2)s + 1}{R_1R_2Cs + R_2} \quad (2.2)$$

Where s is a Laplace complex variable.

2.4 Relaxation model

Studies indicate that the response of the ionic polymer strongly depends on its backbone polymer and ionic content [1, 2], especially the counter ion. Basically, they can be divided to two categories based on the cation size.

(a) Small cation such as Li^+ , Na^+ and K^+

(b) Large cation such as alkyl ammonium ions.

The ionic polymer with small cation has quick response to the applied voltage and slow back relaxation. The ionic polymer with large cation responds slowly to applied voltage but with no relaxation. It is believed that the small cations move easier over the polymer backbone. The fast movement of the cations towards the cathode together with associated water molecules results in an initial quick bending toward to the anode. This response is followed with a relaxation that may be caused by water leakage resulting from a high pressure layer near the cathode toward to the anode through channels in the polymer backbone. The process stops when water equilibrium is established. On the contrary, large cations migrate significantly slower and present slow reaction to the electric field. Thus, there no relaxation for the ionic polymer with large cations.

Since the ionic polymer with small cations under a step input voltage show a slow relaxation towards the cathode after a quick bending towards anode. This phenomenon was considered and modeled using a simple lead network of

$$\frac{u_i}{Q_i} = K \frac{s+z}{s+p}, p > z \quad (2.3)$$

where u_i is a bending moment applied to the ionic polymer segment i and K , z , and p are three parameters that can be fit using the experimental data. Here, K is the gain and z and p are zero and pole of the network. K is related with the bending effect of the charge freshly moving to the electrode and $1/p$ is a relaxation time constant and the magnitude of z reflects the bending effects of the charge in the equilibrium state. Considering the fact that the bending effect due to freshly moving charge is larger than the one in the equilibrium state, the magnitude of z is smaller than p .

The RC model and relaxation model of the IPMC can be combined to the following linear model that relates the input voltage V_i and the bending moment u_i of segment i as

$$\frac{u_i}{V_i} = \frac{\frac{K}{R}(s+z)}{s^2 + (\frac{1}{R_1 C} + p)s + \frac{p}{R_1 C}} \quad (2.4)$$

2.5 Finite element modeling of segment ionic polymer

The finite element method is used to describe the dynamics of the single and segmented ionic polymer strip method is which is as composed of finite elements

satisfying Euler-Bernoulli's beam theory. The displacement of any point on the arm is described in terms of nodal displacements [12]. The position and velocity vectors of a point on the beam is,

$$P = [x \quad w]^T \quad (2.5)$$

$$\dot{P} = [0 \quad \dot{w}]^T \quad (2.6)$$

where x and w are nodal displacements. The ionic polymer is divided into n elements and each has a local coordinate x_i along the neutral axis of the ionic polymer (in the global coordinates) and has a length of L_i . There are $(n+1)$ nodes, with the nodes of element (i) being nodes (i) and $(i+1)$. This is shown in Figure 2.3

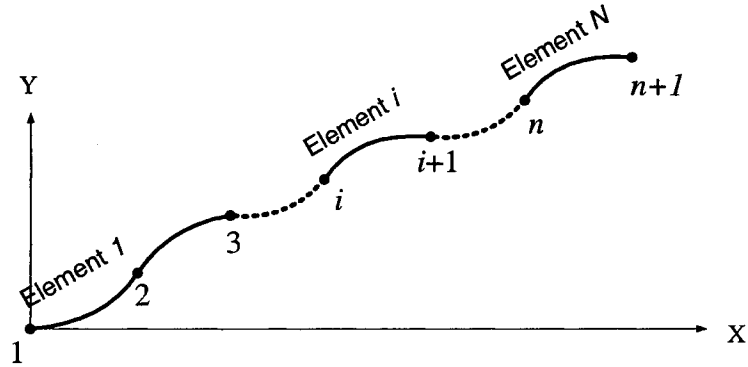


Figure 2.3 shows a schematic of the ionic polymer.

The displacement of any point in element i , shown in Figure.2.4, is described using the nodal displacement and slope of nodes i and $i+1$ as follows:

$$w = Nq_i = [N_1 \ N_2 \ N_3 \ N_4] \begin{Bmatrix} w_i \\ \phi_i \\ w_{i+1} \\ \phi_{i+1} \end{Bmatrix} \quad (2.7)$$

where w_i and ϕ_i are the nodal displacement and slope of node i respectively and N 's are called the *shape functions* which are shown below,

$$\begin{aligned} N_1 &= \frac{1}{L_i^3} (2x_i^3 - 3x_i^2 L_i + L_i^3) \\ N_2 &= \frac{1}{L_i^3} (x_i^3 L_i - 2x_i^2 L_i^2 + x_i L_i^3) \\ N_3 &= \frac{1}{L_i^3} (-2x_i^3 + 3x_i^2 L_i) \\ N_4 &= \frac{1}{L_i^3} (x_i^3 L_i - x_i^2 L_i^2) \end{aligned} \quad (2.8)$$

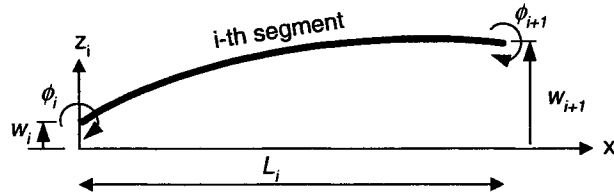


Figure 2.4 i-th segment illustrating nodal displacement

Velocity of any point in element i is

$$\dot{P} = N\dot{q}_i \quad (2.9)$$

The kinetic energy of the element is

$$KE_i = \frac{1}{2} \int_0^{L_i} \rho_i \dot{P}^T \dot{P} dx_i \quad (2.10)$$

where, ρ_i is the combined density of the electrode and the electrolyte between the electrodes per unit length of element i . Substituting the Eq (2.9) to Eq (2.10)

$$KE_i = \frac{1}{2} \int_0^{L_i} \rho_i \dot{q}_i^T N^T N \dot{q}_i dx_i \quad (2.11)$$

By defining 4×4 mass matrix m_i , Eq (2.11) is expressed as

$$KE_i = \frac{1}{2} \int_0^{L_i} \rho_i \dot{q}_i^T m_i \dot{q}_i dx_i \quad (2.12)$$

$$\text{where } m_i = \int_0^{L_i} \rho_i N^T N dx_i \quad (2.13)$$

The mass matrix m_i become

$$m_i = \begin{bmatrix} \frac{13}{35} \rho_i L_i & \frac{11}{210} \rho_i L_i^2 & \frac{9}{70} \rho_i L_i & -\frac{13}{420} \rho_i L_i^2 \\ \frac{11}{210} \rho_i L_i^2 & \frac{1}{105} \rho_i L_i^3 & \frac{13}{420} \rho_i L_i^2 & -\frac{1}{140} \rho_i L_i^3 \\ \frac{9}{70} \rho_i L_i & \frac{13}{420} \rho_i L_i^2 & \frac{13}{35} \rho_i L_i & -\frac{11}{210} \rho_i L_i^2 \\ -\frac{13}{420} \rho_i L_i^2 & -\frac{1}{140} \rho_i L_i^3 & -\frac{11}{210} \rho_i L_i^2 & \frac{1}{105} \rho_i L_i^3 \end{bmatrix} \quad (2.14)$$

The potential energy of an element i assuming uniform beam geometry is

$$PE_i = \frac{1}{2} \int_0^{L_i} \frac{1}{EI_i} \left(EI_i \frac{\partial^2 w}{\partial x_i^2} + u_i \right)^2 dx_i \quad (2.15)$$

where EI_i is the product of Young's modulus of elasticity by the cross-sectional area moment of inertia for the equivalent beam of an element i .

From the Eq (2.15) the stiffness matrix k_i of the element i is defined as

$$k_i = \int_0^{L_i} EI_i \left(\frac{\partial^2 N}{\partial x_i^2} \right)^T \left(\frac{\partial^2 N}{\partial x_i^2} \right) dx_i \quad (2.16)$$

Using Eq (2.8) The complete stiffness matrix is

$$k_i = \begin{bmatrix} \frac{12EI_i}{L_i^3} & \frac{6EI_i}{L_i^2} & -\frac{12EI_i}{L_i^3} & \frac{6EI_i}{L_i^2} \\ \frac{6EI_i}{L_i^2} & \frac{4EI_i}{L_i} & -\frac{6EI_i}{L_i^2} & \frac{2EI_i}{L_i} \\ -\frac{12EI_i}{L_i^3} & -\frac{6EI_i}{L_i^2} & \frac{12EI_i}{L_i^3} & -\frac{6EI_i}{L_i^2} \\ \frac{6EI_i}{L_i^2} & \frac{2EI_i}{L_i} & -\frac{6EI_i}{L_i^2} & \frac{4EI_i}{L_i} \end{bmatrix} \quad (2.17)$$

Using Lagrangian dynamics, the equations of motion for an element i are,

$$\frac{d}{dt} \left(\frac{\partial (KE_i)}{\partial \dot{q}_i} \right) - \left(\frac{\partial (KE_i)}{\partial q_i} \right) + \left(\frac{\partial (PE_i)}{\partial q_i} \right) = 0 \quad (2.18)$$

The terms with u_i are moved to the right hand side of the equation. They correspond to the force matrix of a distributed moment that is replaced by two concentrated moments at the two nodes. The equation can be expressed in a matrix form as,

$$m_i \ddot{q}_i + k_i q_i = B_i u_i \quad i = 1 \dots n \quad (2.19)$$

where m_i and k_i are shown in Eq. (2.12) and Eq. (2.17) respectively and $B_i = [0 \ -1 \ 0 \ 1]$

2.6 State space model development

To develop the combined state space model for an entire ionic polymer length of n segments Eq. (2.4) and (2.20) should be expanded. First, the RC relaxation model of each segment in Eq.(2.4) can be written as

$$\frac{u_i}{V_i} = \frac{\frac{K}{R}(s+z)}{s^2 + \left(\frac{1}{R_1 C} + p\right)s + \frac{p}{R_1 C}} = \frac{b_{i1}s + b_{i0}}{s^2 + a_{i1}s + a_{i0}} \quad (2.20)$$

$$\text{where } b_{i1} = \frac{K}{R_1}, b_{i0} = \frac{K}{R_1} z, a_{i1} = \left(\frac{1}{RC_1} + p \right), a_{i0} = \frac{p}{R_1 C}$$

Eq (2.20) can be transformed back to time domain as

$$\ddot{u}_i + a_{i1}\dot{u}_i + a_{i0}u_i = b_{i1}\dot{V}_i + b_{i0}V_i, \quad i = 1 \cdots n \quad (2.21)$$

To combine the RC and relaxation model with the equations of motion (2.20), we introduce two new variables z_{i1} and z_{i2} for element i ,

$$\dot{z}_{i1} = z_{i2} \quad (2.22)$$

$$\dot{z}_{i2} = -a_{i1}z_{i2} - a_{i0}z_{i1} + V_i$$

Then, u_i of Eqs.(2.21) can be expressed in terms of these new variable z_{i1} and z_{i2} as

$$u_i = b_{i0}z_{i1} + b_{i1}z_{i2}, \quad i = 1 \cdots n \quad (2.23)$$

Eq. (2.22) and (2.23) can be expanded for the entire ionic polymer of n segments as

$$\begin{aligned} \dot{Z} &= \begin{bmatrix} 0_{n \times n} & 0 & -a_{11} & 0 & 0 \\ -a_{10} & \ddots & 0 & 0 & \ddots & 0 \\ 0 & \ddots & 0 & 0 & \ddots & 0 \\ 0 & 0 & -a_{n0} & 0 & 0 & -a_{n1} \end{bmatrix} Z + \begin{bmatrix} 0_{n \times n} \\ I_{n \times n} \end{bmatrix} V \\ &\equiv A_z Z + B_v V \end{aligned} \quad (2.24)$$

where $Z = \{z_{11} \ z_{21} \cdots z_{n1}, \ z_{12} \ z_{22} \cdots z_{n2}\}^T \in \mathbb{R}^{2n}$ and $V = \{V_1 \ V_2 \cdots V_n\}^T \in \mathbb{R}^n$ is an input voltage vector. Also Eq (2.22) can be expanded for an entire ionic polymer strip of n segments as,

$$u = \begin{Bmatrix} u_1 \\ \vdots \\ u_n \end{Bmatrix} = \begin{bmatrix} b_{10} & 0 & 0 & b_{11} & 0 & 0 \\ 0 & \ddots & 0 & 0 & \ddots & 0 \\ 0 & 0 & b_{n0} & 0 & 0 & b_{n1} \end{bmatrix} Z \equiv B_u Z \quad (2.25)$$

The dynamic model for the segment i shown in (2.19) need to be expanded for an entire ionic polymer of n segments. Matrix equations (2.19) for each segment can be assembled after expansion as

$$M_e \ddot{q}_e + K_e q_e = B_e u \quad (2.26)$$

where $q_e = \{w_2 \phi_2 \ w_3 \phi_3 \ \cdots w_{n+1} \phi_{n+1}\}^T \in \Re^{2n}$ and a bending moment vector

$u = \{u_1 \ u_2 \ \cdots u_n\}^T \in \Re^n$. It should be noted that $\{w_1 \phi_1\}$ is eliminated from q_e since the first node has zero boundary conditions. Now the state space model of the entire ionic polymer strip can be formulated using (2.19)-(2.21).

By defining a state vector $x = \{q_e \ \dot{q}_e \ Z\}^T \in \Re^{6n}$, (2.19)-(2.21) can be written as,

$$\begin{aligned} \dot{x} = \begin{Bmatrix} \dot{q}_e \\ \ddot{q}_e \\ \dot{Z} \end{Bmatrix} &= \begin{bmatrix} 0_{2n \times 2n} & I_{2n \times 2n} & 0_{2n \times 2n} \\ -M_e^{-1} K_e & 0 & M_e^{-1} B_e B_u \\ 0 & 0 & A_z \end{bmatrix} x + \begin{bmatrix} 0 \\ 0 \\ B_v \end{bmatrix} V \\ &\equiv Ax + BV \end{aligned} \quad (2.28)$$

Eq (2.26) can be used for designed a control law for the segmented ionic polymer strip for various applications in end-effectors and underwater propulsor design.

CHAPTER 3

EXPERIMENT SETUP

This section describes the methods and hardware used to generate the inputs applied to the ionic polymer and to measure dynamic response of the ionic polymer. These inputs and measurements will be referred in later sections in this chapter. The Figure 3.1 shows basic Illustration of the Experimental Setup.

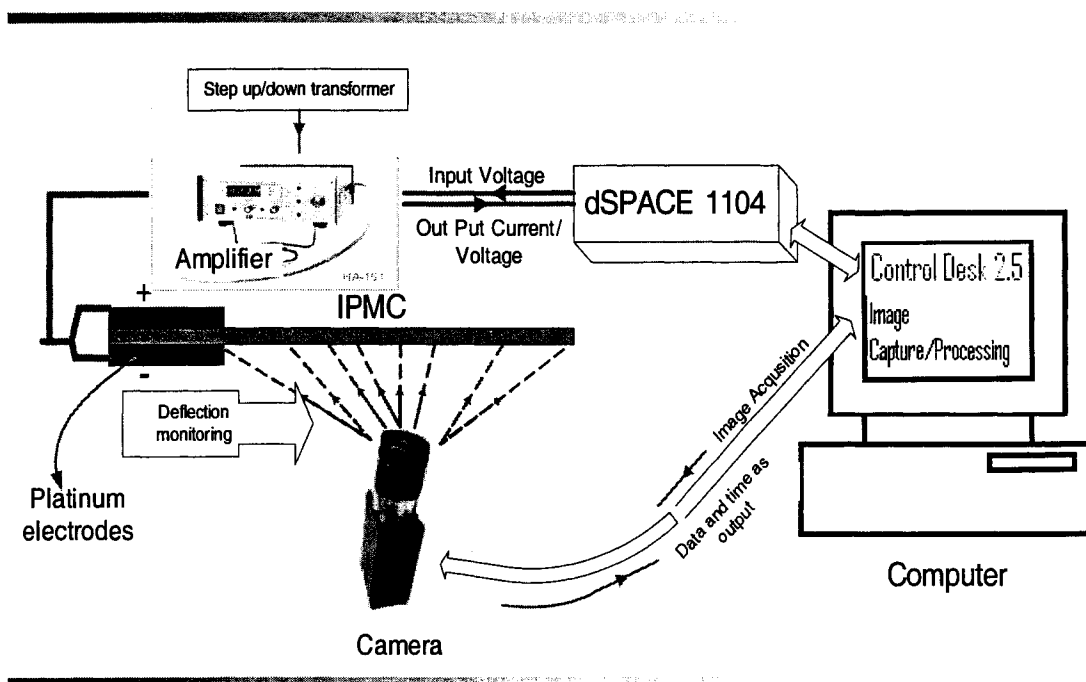


Figure 3.1 Schematic diagram illustrating basic experimental setup

As shown in the Figure 3.1, the ionic polymer was clamped between a pair of platinum electrodes. When the ionic polymer is in the air the deionized water (1-Butyle-3-methylimidazolium-hexafluorophosphate) was brushed on the ionic at approximately one minute intervals-frequently enough to keep the surface of the polymer wet. When the polymer is not in use, it is stored in sodium hydroxide solution to avoid hydration. As the experiment was performed both in air and water an aquarium with a holding frame was used to hold the polymer. Actual Experiment setup is shown in Figure 3.2 and the holding device with single segment polymer is shown in Figure 3.3

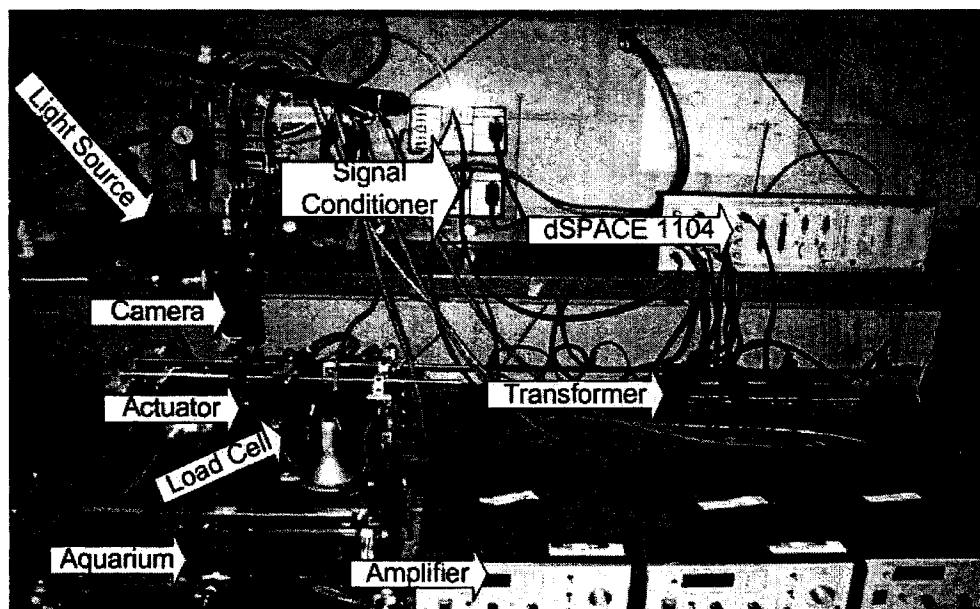


Figure 3.2 Actual experiment setup

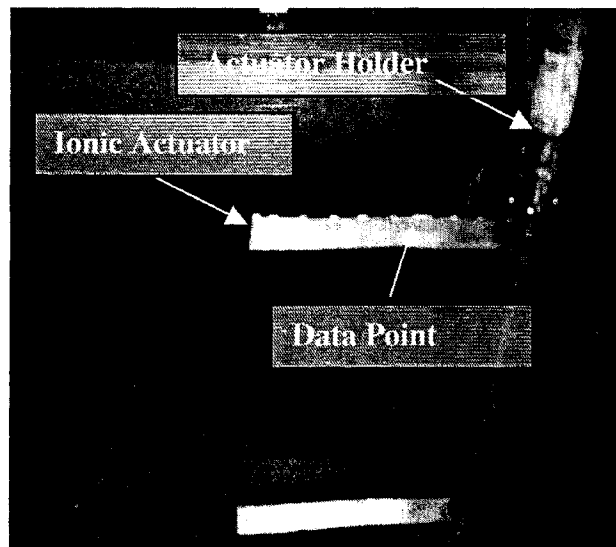


Figure 3.3 IPMC setup with polymer holding Device

3.1 Experiment description

Experimental setup mainly consisted of the following

- dSPACE 1104 system (Real time controller prototyping system)
- Three programmable bi-polar power amplifiers for model (HA-151 by Hokuto Denko)
- Three step up and down transformers model (VC-100J by Power bright) for giving power input amplifier.
- Camera (A602f by BASLER)
- 10 gram load cell with TMO-1 Signal conditioning circuit for force measurement.
- Open top aquarium
- Actuator holder
- Platinum electrodes

Following software's were used for Data Acquisition

- DSPACE Control Desk Version 2.5
- Simulink , Image acquisition and Image processing Tool box in Matlab 6p5

3.2 Control signal for ionic polymer

Voltage inputs for the time domain experiments were generated using D/A converters output channels of the dSPACE 1104. Voltage output from the dSPACE was amplified and conditioned using programmable Bi-polar power amplifiers. The output voltage and current from the amplifier was measured by accessing DAC (Digital to Analog) channel of dSPACE system.

3.3 Blocking force measurement of ionic polymer

The 10 gram load cell manufactured by Transducer Techniques was used to measure the blocking force of the tip of the ionic polymer. The load cell precision, repeatability, and linearity were 0.05mN. The force measurement was also relatively noisy, with typical noise level of 0.02mNrms. The force between the ionic polymer and the load cell sensing element was transferred through a nylon screw that was screwed into the tapped hole provided in the load cell sensing element. The Figure 3.4 illustrates the load cell setup with ionic polymer. The output of the load cell is voltage connected to DAC channel of the dSPACE system for monitoring the blocking force generated by the ionic polymer.

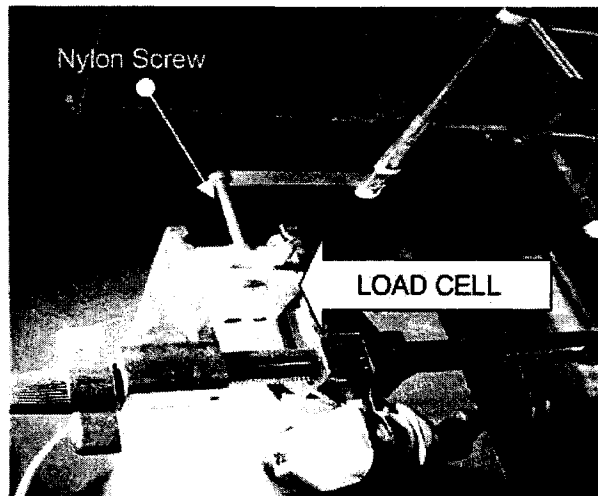


Figure 3.4 Load Cell Setup

3.4 Deflection measurement of the ionic polymer

Deflection monitoring of the ionic polymer were made using BASLER A602f digital video camera. The camera is capable of frame rates up to 100 fps (frames per second). A frame rate of 3 fps was used for the experiment reported in this work. Ten equally spaced small 'dots' of metallic silver color on the polymer edge acted as targets for the Image Processing toolbox. For post processing of the acquired images, the Image Processing tool box was used to create a time history of the target position. The resolution achieved in a particular experiment depends on many factors, such as lighting, target size and shape, and lens quality. Thus the Image Acquisition Tool box and Image Processing tool box of Matlab provided means by which to measure large ionic polymer deflection.

Appendix A provides the specifications of the ionic polymer and instruments used in this experiment.

3.5 Interfacing image acquisition and dSPACE 1104

The dSPACE controller and the Matlab toolbox based vision system are two different systems and we need to synchronize two system for various the various data acquisition and control applications. This synchronization can be achieved by a program that triggers both dSPACE and vision acquisition system. For this purpose we use a feature in dSPACE called MLIB/ MTRACE.

Programming MATLAB-dSPACE Interface libraries gave us an access to dSPACE real-time processor hardware from the MATLAB workspace. MLIB/MTRACE functions can be called from the MATLAB Command Window or from MATLAB M files. Thus the powerful numerical tools like Image Acquisition running under MATLAB can be used in combination with MLIB/MTRACE for:

- Analyzing real-time data
- Test automation
- Optimizing control algorithms

MLIB/MTRACE provides basic functions for reading and writing data to dSPACE processor boards and other functions for generating interrupts, setting the processor state, and getting processor status information. MLIB/MTRACE functions are used to modify parameters online and to send sequences of test data to real-time applications. MLIB/MTRACE ideally complements the software environment, which consists of MATLAB, Simulink, Real-Time Workshop, and the dSPACE tools RTI and Control Desk. Figure 3.5 shows the illustration of how dSPACE from MATLAB M files via MLIB/MTRACE

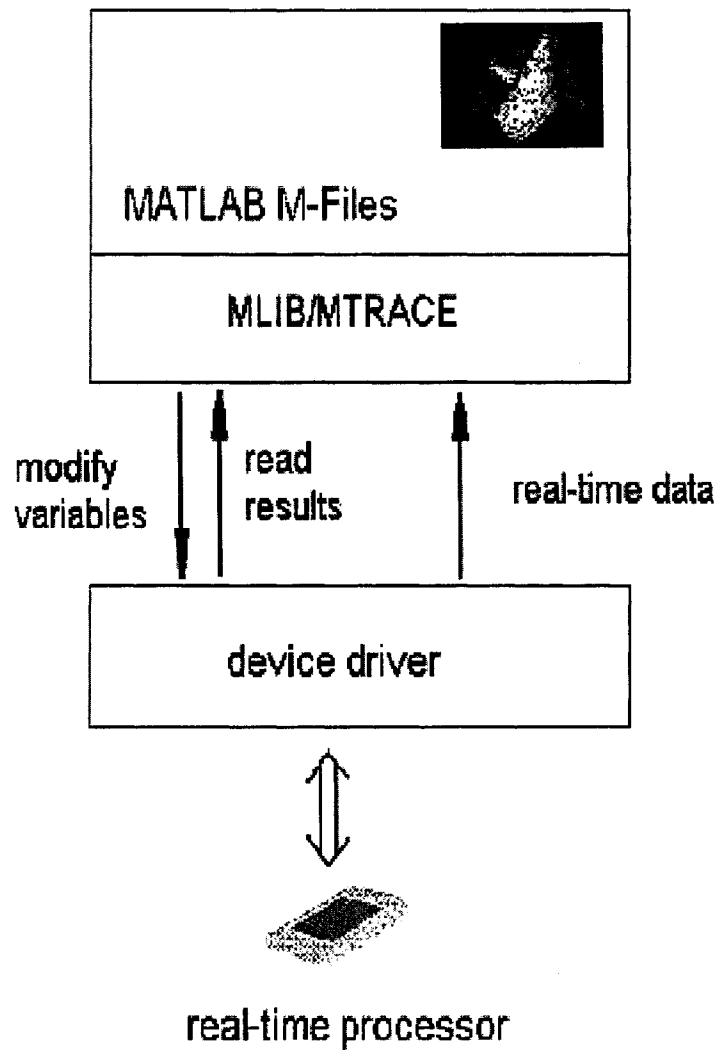


Figure 3.5 Interfacing of MATLAB with Real time Processor of dSPACE

The m-file used to trigger both Image acquisition and dSPACE is provided in Appendix-B

3.6 Image processing

After the target images are acquired, those images need to be processed to calculate the position of each target points marked on the polymer. This was a technique where we carried out set of numeric operations to process the images acquired and to perform required operation. We could extend the capabilities of the Image Processing Toolbox by writing our own M-files, which performed following tasks shown in Figure 3.6

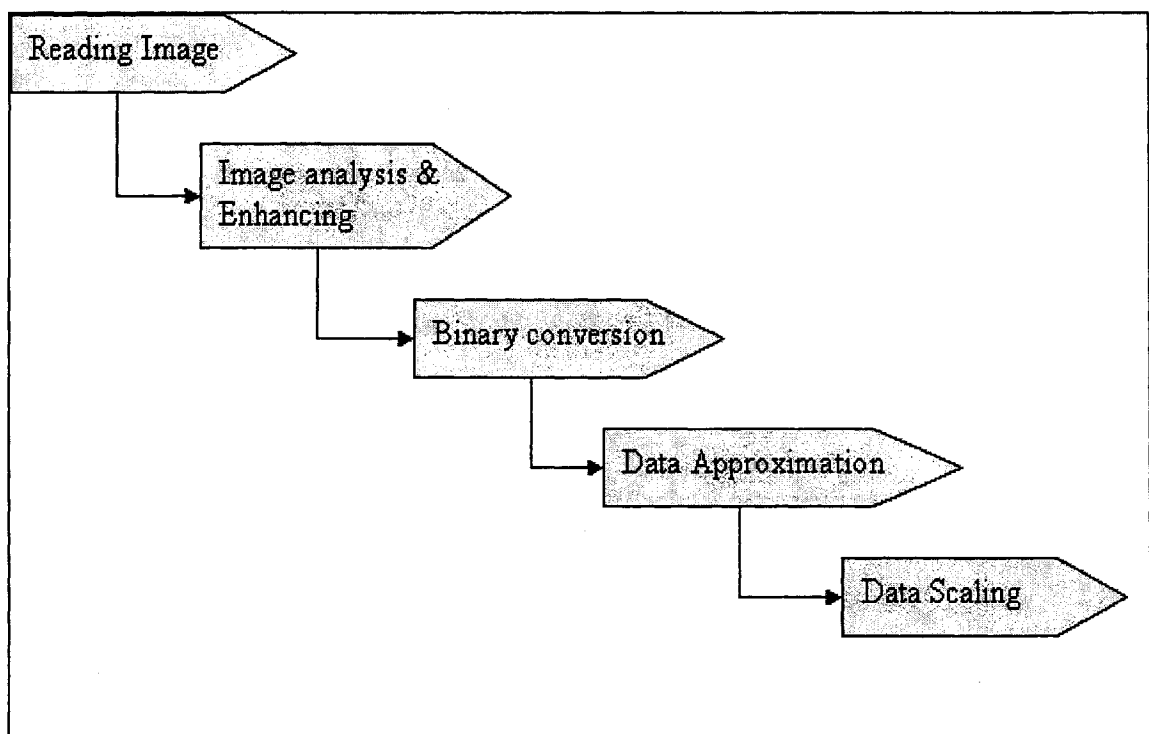


Figure 3.6 Tasks of image processing

Each task in Figure 3.6 is summarized in this section.

3.6.1 Image reading

Image reading is a process of reading an image from any supported graphics image file format, in any of the supported bit depths. Most image file formats use 8 bits to store pixel values. When these are read into memory, MATLAB stores them as a class `uint8` (unsigned positive integer). For the file formats that support 16-bit data, PNG and TIFF, MATLAB stores the images as class `uint16`. Figure 3.7 shows the sample image that has been read by MATLAB.

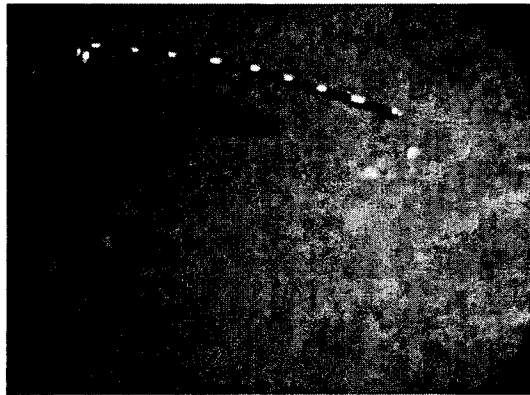


Figure 3.7 Sample image

3.6.2 Image enhancing & analysis

Image Enhancing and analysis techniques return information about the structure of an image. After analyzing the image we increase the intensity of the image by using default functions that enhances the contrast of images by transforming the values in an intensity image so that the histogram of the out space image approximately matches a

specified histogram (uniform distribution by default).Figure 3.8 shows a sample of image enhancement.

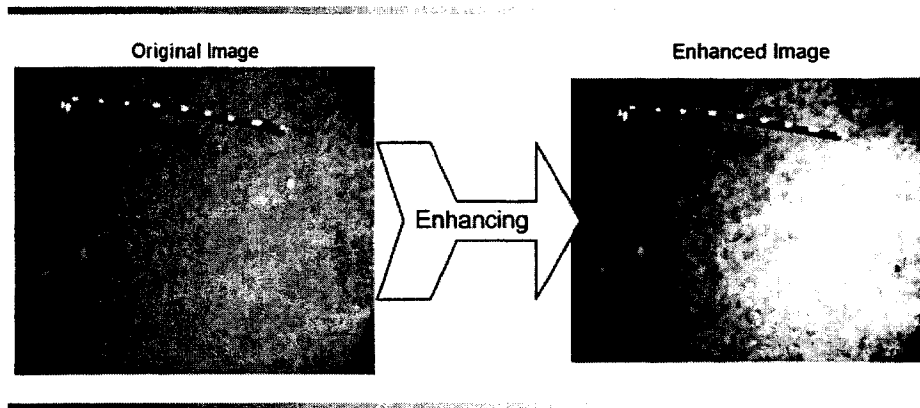


Figure 3.8 Image enhancing

3.6.3 Binary conversion

Followed by the image enhancement by adjusting intensity of the images, the next task is to convert the enhanced images to the binary format. The binary images are the images that contain only 0's and 1's. Pixels with the value 0 are displayed as black; pixels with the value 1 are displayed as white. For the toolbox to interpret the image as binary, it must be of class logical Image. Figure 3.9 shows the sample of binary image.

Black and white Image

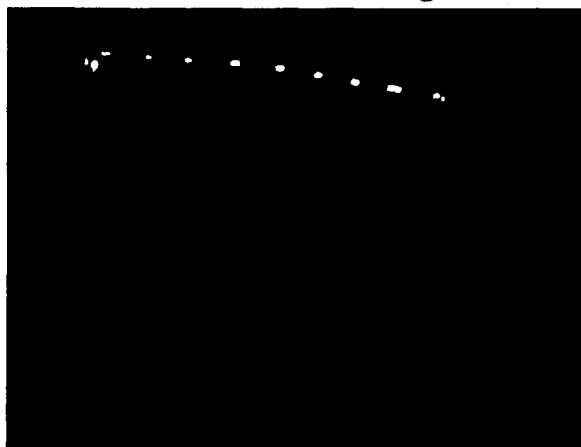


Figure 3.9 Binary image

3.6.4 Data approximation

In the transformed binary images the white regions which show the position of target points would be our area of interest. Before approximation we label every 'dot' or white spot to access individual dots later by labeled number. To approximate the data region (dot) as single point we calculated the centroid of the white region and considered that centroidal point as the actual position of data.

3.6.5 Data scaling

Reference scale of the image data was the pixel number which is needed to be scaled in meters. This scaling was done using the reference images with known dimension and each image was scaled using that scaling. In the proposed setup, 100 pixel length is equivalent to 12 mm of actual object. Taking the above scaling into consideration, the deflection analysis of ionic polymer was done.

The m-file used to Process the Image in the above discussed steps is provided in Appendix B

3.7 Pre chemical processing of ionic polymer

Ionic polymer's gets hydrated quickly in the air and so in order to keep the surface of the polymer wet, deionized water (1-Butyle-3-methylimidazolium-hexafluorophosphate) is to be brushed on the actuator at approximately one minute intervals-frequently at the time of experiment. The ionic polymer response can change after some couple of routine experiments and this is due to some organic and metallic impurities.

In order to ensure repeatability in response of the ionic polymer there was the need to remove the organic and metallic impurities which can affect the ionic polymer. To do this there is a sequence of pretreatment process that can remove the organic and metallic impurities.

The pretreatment process was explained in following steps

- First, the ionic polymer has to be cleaned in Distilled water.
- Then immerse the polymer in DI water to swell the membrane for 2 hours
- Boil the membrane in 3% Hydrogen Peroxide (H_2O_2) solution at $80^\circ C$ for 30 minutes. This removes the organic impurities.
- After boiling, the polymer has to be cleaned by rinsing the membrane in DI water.
- Boil the membrane in 1 molar Sulfuric acid (H_2SO_4) at $80^\circ C$ for 40 minutes. This dissolves all the metallic impurities.

- After boiling, the polymer has to be cleaned by rinsing the membrane in DI water again.
- Then the polymer has to be left in Sodium Hydroxide solution for 24 hours.
- Then polymer is ready to use. Water used in the experiment should always be DI water to ensure the proper response of the actuator.

3.8 Integration of vision system with dSPACE

Keeping in view of applying the control law to the system, Next task was to develop vision feed back system. This task has following steps

- Standardize scaling procedure
- Developing Matlab function for Acquisition and Processing
- Synchronize with the existing dSPACE and Image Acquisition System

3.8.1 Standardize scaling procedure

Image processing previously discussed was procedure carried out after the data/video was acquired. Scaling the data points from pixel number to SI units are done considering the reference picture. This method of plotting the data points was found to have more approximation and not viable.

There were many image sensing and scaling techniques that were available which when implemented ensures the accurate scaling of the given image. Due to the complexity involved in understanding and again synchronizing with other systems these could not be implemented.

Hence we came up with scaling system where we fix the distance, angle of vision, focus between ionic polymer and camera as shown in the Figure 3.10. This ensures the specific area of vision at that fixed distance. Using graph paper as field of view an image was collected and calibrated the pixel value. In our case it was image captured is of resolution 680×480 pixels.

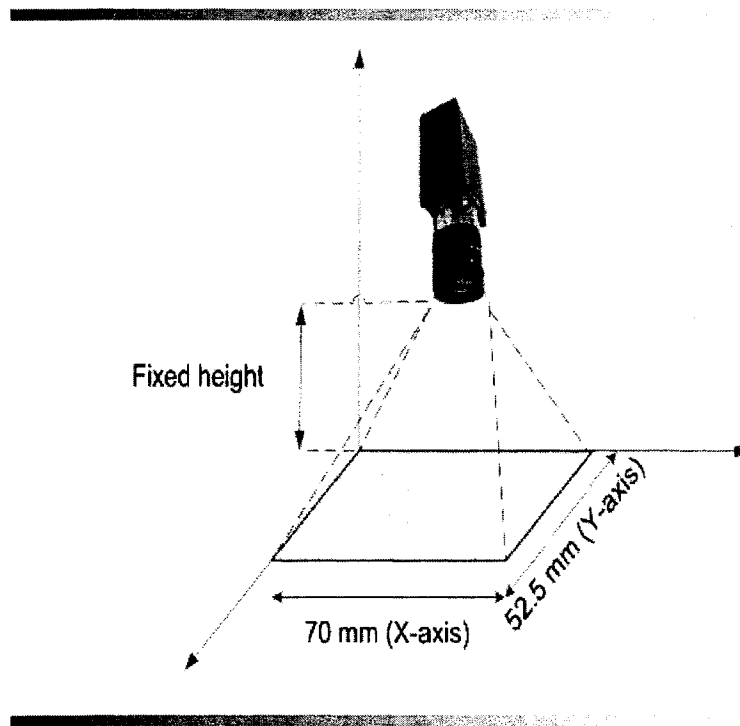


Figure 3.10 Camera positioning

This when scaled to millimeter it would be 70×52.5 mm. Thus each pixel value is equal to .10925 mm. Having fixed the scaling constant, any image captured with the fixed distance, angle of vision, focus can be multiplied with scaling constant to get the data point located in SI system.

Y-axis in the pixel increases from top to bottom as shown in the Figure 3.11. In order to account this simple math operation has been done. After multiplying the y axis pixel value with the scaling constant the resultant is subtracted from the length of the Y-axis (52.5). Thus value in y-axis increases from origin.

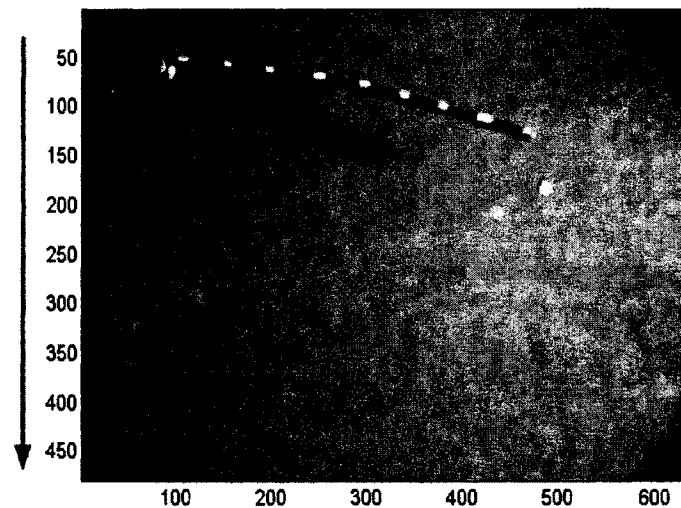


Figure 3.11 Arrow direction indicating the y-axis increases from top to bottom

3.8.2 Developing function for acquisition and processing

The next task was to develop the function. This function when called should carry out following options

1. Capture image
2. Process the image to black and white image
3. Find out the point of interest
4. Scale the date point to SI system
5. Give the output as tip point located in SI system.

Capturing and filtering image with reference to highest intensity is same as that was explained in Image Processing Section 3.6. In order to locate the tip point we consider the point with highest x-axis value. So after labeling the points in the image, the data point with highest x-coordinate value will be considered as our point of interest. Thus tip of the ionic polymer is recognized by the camera and the output of the function would be tip of the ionic polymer located in co-ordinate axis in millimeters. The above is shown in the following Figure 3.12

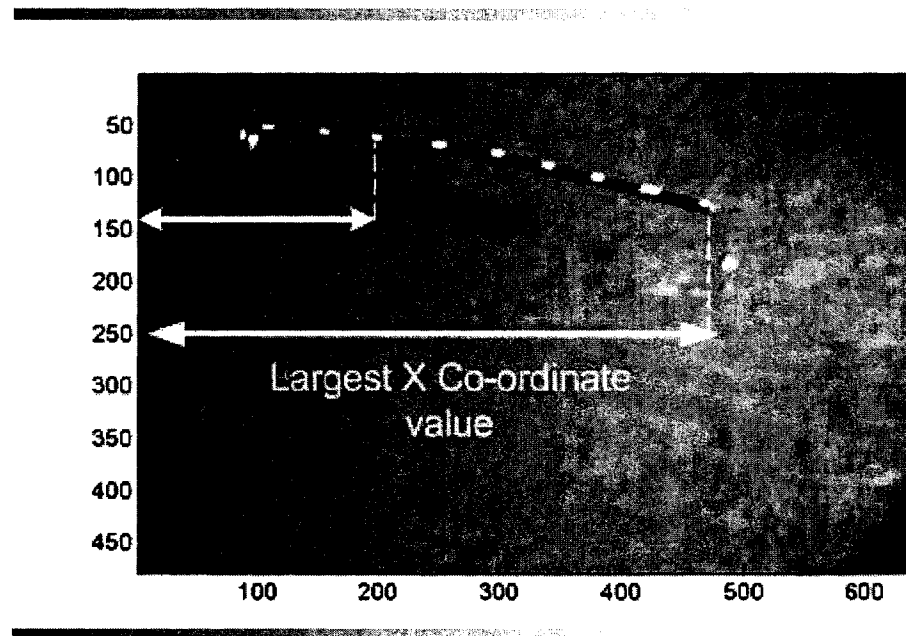


Figure 3.12 Finding the tip displacement by considering the data point with highest 'x' value

3.8.3 Synchronize with the existing dSPACE and image acquisition system

To summarize above we program the above tasks under one function and call that function for every given voltage at that instant to monitor the response of the ionic polymer for given voltage. Thus synchronizing the dSPACE and image acquisition system to study open loop response of the system.

CHAPTER 4

RESULTS AND DISCUSSION

4.1 Experimental results

This section explains the types of experiments conducted and their results. As explained in Chapter 3, the experimental setup holds good for different types of data acquisition. The primary task was to monitor deflection of ionic polymer for input step voltage using a video camera and validate the responses obtained from the computer simulated result. Figure 4.1 shows the ionic polymer holder that is designed using Solid Works and manufactured using Dimension SSS 3D rapid prototyping machine.

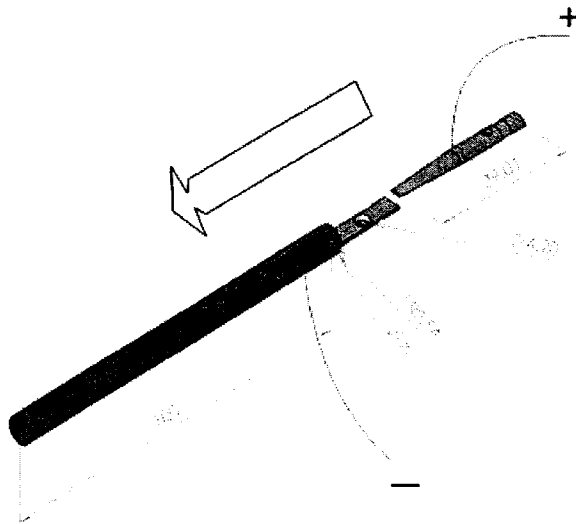


Figure 4.1 Ionic polymer holder

The ionic polymer used in this experiment has to undergo pre-chemical treatment (Sec 3.7) discussed in Chapter 3. This would ensure the better repeatability in response of the ionic polymer. Two platinum electrode of dimension $2\text{mm} \times 10\text{mm} \times 0.1\text{mm}$ (length \times breadth \times height) is used to hold the ionic polymer of $50\text{mm} \times 10\text{mm} \times .29\text{mm}$ (length \times breadth \times height). The ionic polymer used in our experiments is provided by the Active Material Research laboratory, University of Nevada Reno. This ionic polymer is made of Nafion 117 based polymer with H^+ cation. Ionic polymer is clamped between the platinum electrodes as shown in Figure 3.3. This electrode receives the input voltage from the amplifier (HA 151). The amplifier receives the programmed real time voltage signal from the real time controller (dSPACE DS 1104 controller board). The acceptable range of the voltage that can be supplied to the ionic polymer is -4 to 4 Volts. The output current and voltage can be monitored from the amplifier output.

In an effort to understand the deflection response of the ionic polymer for various input voltages, the ionic polymer is subject to various step voltages. These experiments were conducted in air and to prevent the polymer from dehydrating during experiment, deionized water was brushed on them at one minute interval on their surface. The step input of 2.5V, 3V, 3.5V and 4 Volts are given to ionic polymer deflection and the current plots are plotted respectively.

4.1.1 Deflection response for 2.5 Volt step input

The amplifier used in this experiment has 2 analog output channels, voltage (potential output) and current. This amplifier is also called Potentiostat / Galvonostat that can used as either voltage or current controlled amplifier.

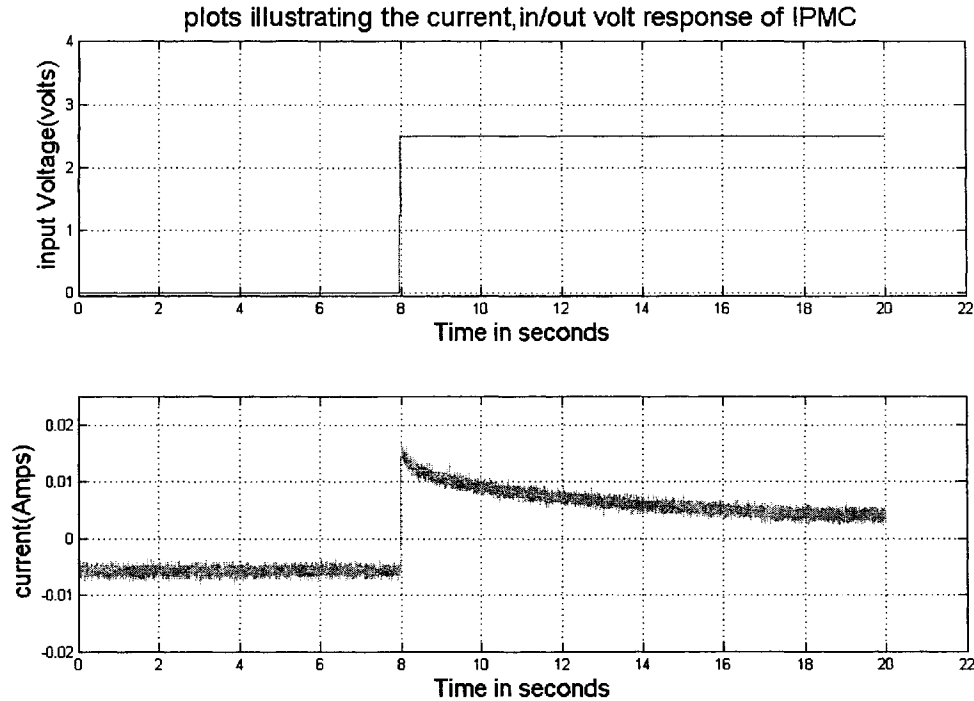


Figure 4.2 Current response of the ionic polymer for 2.5 V step input

The output of the amplifier is also connected to the ADC channel of real time interfacing (dSPACE DS 1104) system for monitoring purpose. The Figure 4.2 shows current response of the ionic polymer for 2.5 Volts input. Thus all input signals were measured and recorded using the dSPACE. The deflection data has been captured using a BASLER camera and processed to analyze the response of the ionic polymer for the given voltage input. Figure 4.3 shows the deflection response of ionic polymer. The dots in Figure 4.3 along the length of the ionic polymer are data points marked on the ionic polymer as targets of the vision system. The tip displacement curve in the Figure 4.3 indicates that there are net displacements of around 13 mm vertically and 2 mm horizontally.

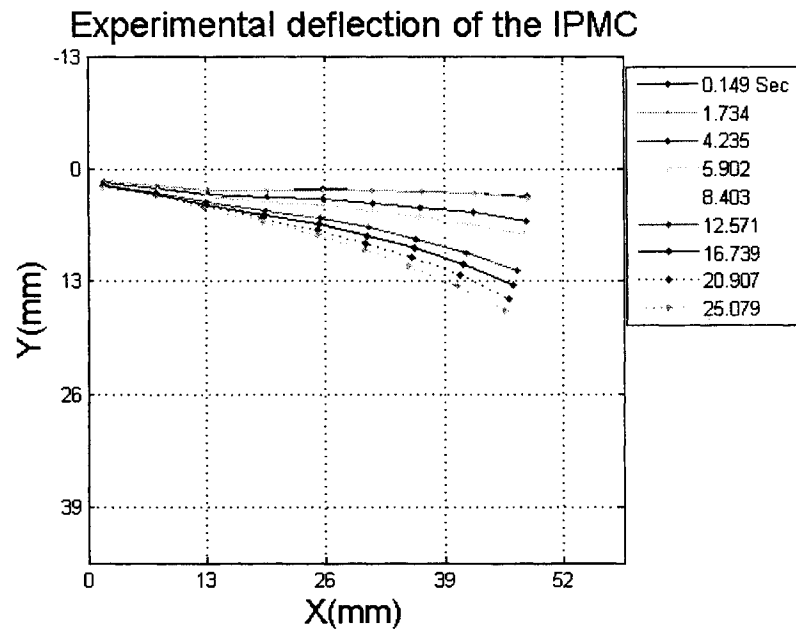


Figure 4.3 Experiment deflection of the ionic polymer for 2.5 volts step input.

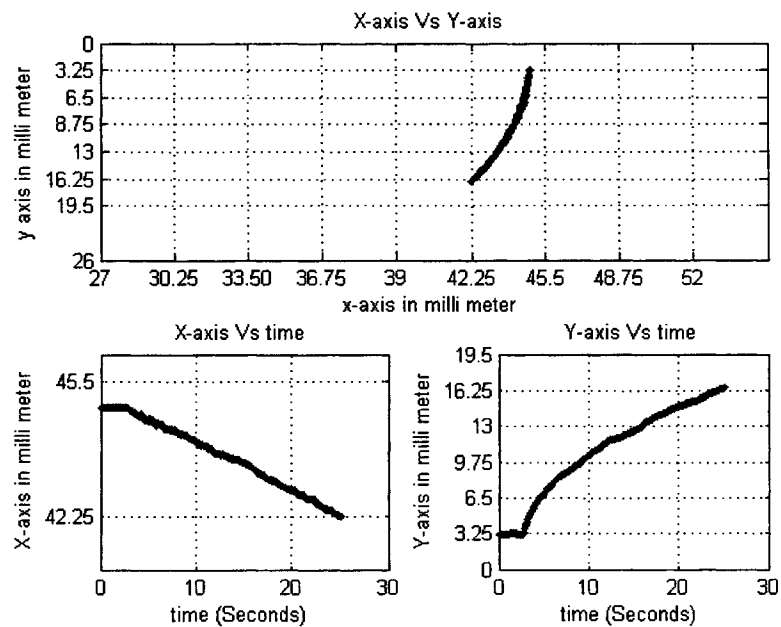


Figure 4.4 Tip displacement curves of the ionic polymer for 2.5 volts

4.1.2 Deflection response of ionic polymer for 3 Volt Step Input

Similar experiment was conducted with 3 volts as an input. Figure 4.5, Figure 4.6 and Figure 4.7 indicate current response, deflection response and tip displacement respectively.

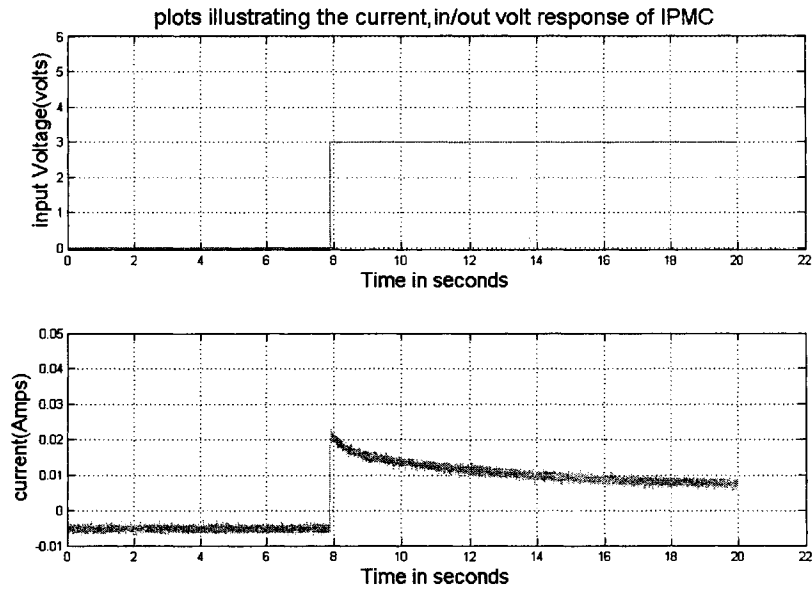


Figure 4.5 Current response of the ionic polymer for 3 V step input

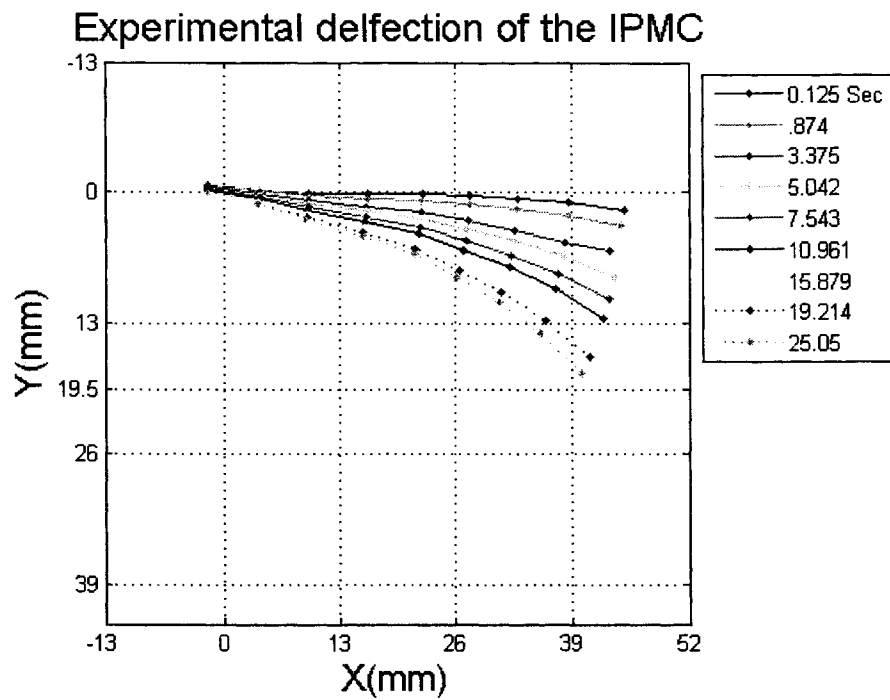


Figure 4.6 Experiment deflection of the ionic polymer for 3 Volts step input.

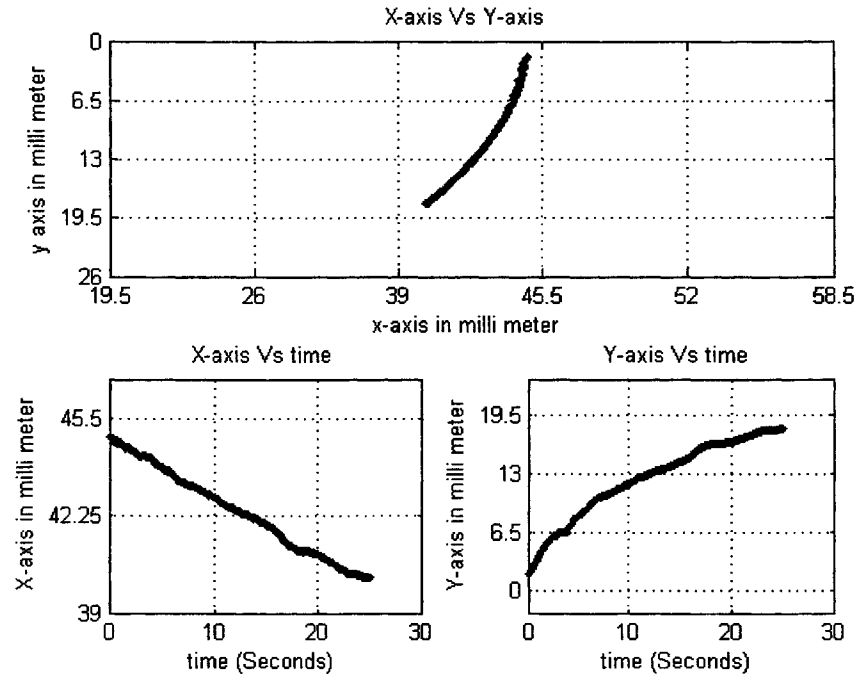


Figure 4.7 Tip displacement curves of the ionic polymer for 2.5 volts

4.1.3 Additional observations

In the process of analyzing ionic polymer the step input with magnitudes 2.0V, 3.0V, 3.5V and 4V were applied to ionic polymer to observe the current and deflection responses for different input voltages.

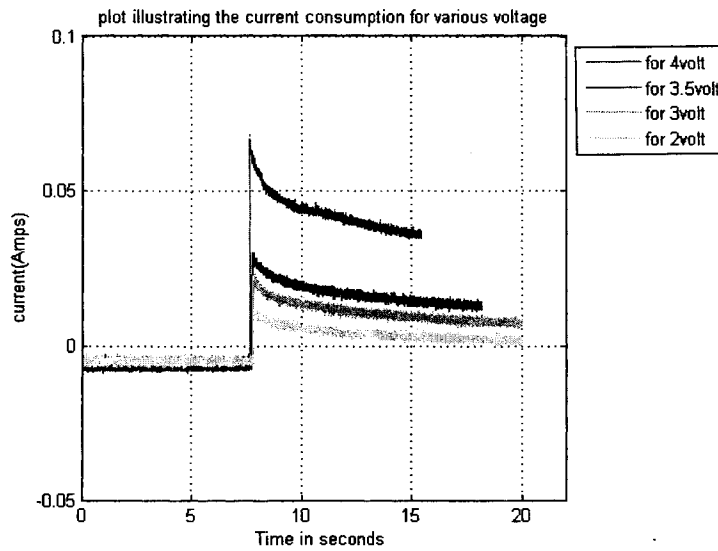


Figure 4.8 Current with 2V,3V, 3.5V and 4V step inputs

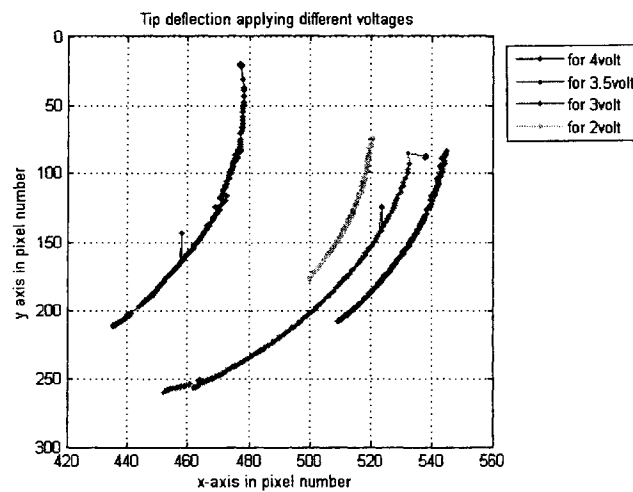


Figure 4.9 Experimental free deflection with 2V, 3V, 3.5V, 4V

These experiments were run for around 20 seconds and the current response was plotted in Figure 4.8. As expected from the clumped RC model in Chapter 2, we obtain the steady state current values proportional to the input voltages after the initial overshoot. It can be also observed that in Figure 4.9 the deflection in Y axis is approximately proportional to the input voltage. In Figure 4.9, it should be noted that tip displacement of ionic polymer with different step inputs do not have same starting point because of intermediate brushing of ionic polymer with deionized liquid to keep the surface of the polymer wet. This brushing disturbs the starting position of the polymer

Figure 4.8 shows that current curve attains stability after certain time, this indicates that after certain time current and force generating bending motion of the ionic polymer is balanced. The fact that the ionic polymer did not continue to bend while constant current was applied supports the above results. As predicted from the clumped RC model in Chapter 2 the current in ionic polymer generates volumetric strain of expansion and contraction.

4.1.4 Blocking force response

The other task was to observe the blocking force. This was measured using 10gm load cell as explained in section 3.3 and Figure 3.4 shows the experimental setup. In order to ensure the contact between the load cell's nylon screw and the tip of the polymer the load cell was placed in such a way that the tip of the polymer was slightly preloaded. These preload constant is accounted and subtracted from the force measurement during post processing.

Based on ion size, the ionic polymer can be classified in two kinds. One is the ionic polymer with small cation and the other is the ionic polymer with large cations. As explained in chapter 2, the ionic polymers with large cation don't exhibit any relaxation as they move slowly towards the cathode resulting in slow bending and less force for applied voltage. The main purpose of ionic polymer with large cationic polymer like alkyl ammonium is to avoid hydration.

Ionic polymer with small cation moves faster and easier on the polymer surface. As they move fast towards cathode they carry water molecule results in an initial quick bending towards the anode. Thus leads to slow relaxation as water leaks from high pressure area towards low pressure area.

Figure 4.10 shows the plot of the blocking force of ionic polymer with different length i.e. 50×10 (Length \times Breadth) and other with 25×10 . Polymers considered in this experiment were polymers with large cations and step input of 3.5V. It is observed that ionic polymer with shorter length (25×10) generates more blocking force than the polymer with longer ionic polymer (50×10). Explanation to this would be the ionic polymer with shorter length is more stiff and the moment generated upon voltage input is distributed in shorter length.

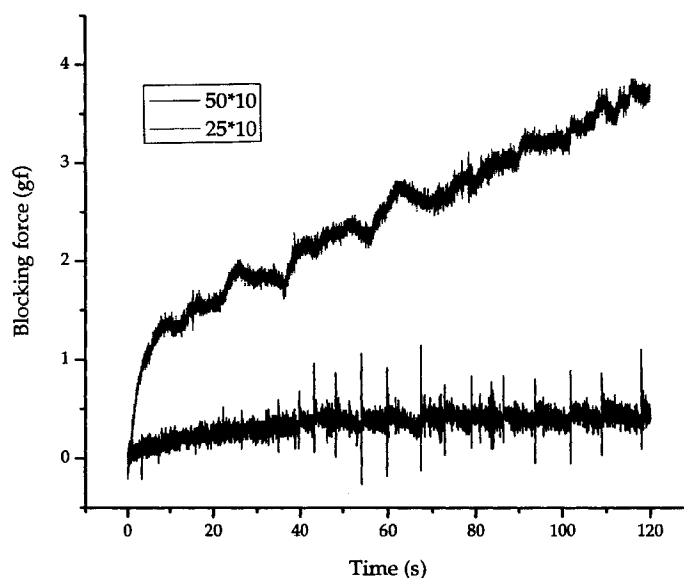


Figure 4.10 Blocking force for two different size of polymer with large cation

In Figure 4.10 it is observed that force plot of the polymer with shorter length (25×10) increases continuously unlike the other polymer (50×10) the reason behind this would be the high power density formed due to short length of polymer

Apart from considering ionic polymer with large cation or small cation of the polymer, the length of the ionic polymer is important parameter to observe relaxation of the ionic polymer. If the ionic polymer's length to width ratio is larger like 5:1 in our case there is no relaxation it can be observed from Figure 4.10

But if the length of the ionic polymer with small cations is short then a slow relaxation is observed. An experiment is conducted to justify above statement. The ionic polymer with small cations (H^+) of 25×10 (L**×**b) is given the step input of 1 volt. Figure 4.11 shows the force response of the ionic polymer to step input of 1 volt. The response time of the bending force is much faster that the case of large ion shown in Figure 4.11.

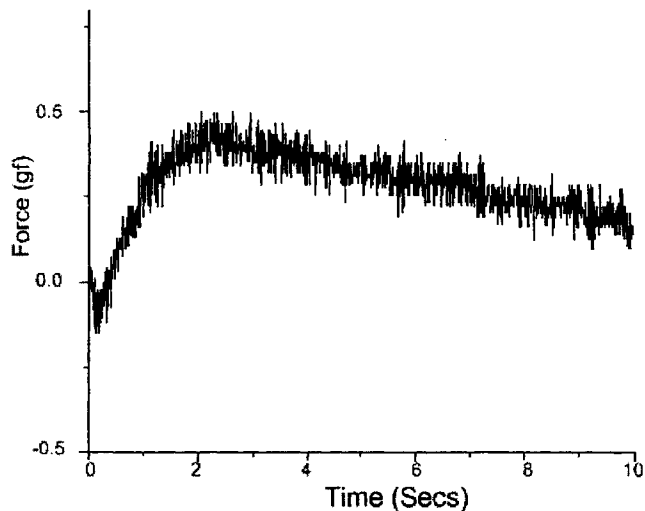


Figure 4.11 Blocking force polymer with small ion

The force recorded in this case is 0.48 gfs. The reported force is referred to the peak value of the force response plot. Similar experiments were conducted with pulse input of amplitudes 4V, 3.5V, 3V and 2.5 V. The pulse period used in these experiments is 20 Secs. The peak force recorded in these experiments is tabulated below.

Table 4-1 Voltage Vs force

Voltage (Volts)	Current (Amps)	Force (gf)
4	0.025	0.075
3.5	0.020	0.05
3	0.016	0.038
2.5	0.007	0.015

4.1.5 Experiments conducted with segmented ionic polymer

A segmented ionic polymer consists of a number of independently electroded sectors along the length of the polymer. Each segment of the ionic polymer can be made by carving the surface of the ionic polymer. This type of actuator gives the scope of controlling each segment independently, achieving snake like wavy motion.

The task was to design the experimental setup. The patterned segment on strip of ionic polymer is shown in Figure. 4.11

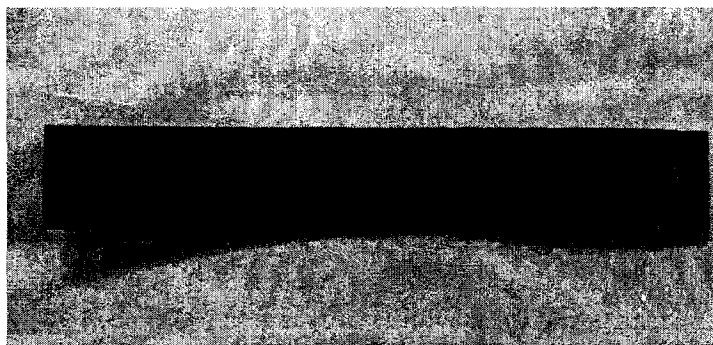


Figure 4.12 Segmented ionic polymer

Electric insulation of each segment was done to verify each segment has independent electrodes. To apply input voltage directly to each segment we used three connectors and thin wire (0.1 mm) touching each segment directly. The connectors used are 'C' shaped clamps that hold the electrodes and segment ionic polymer together as shown in Figure 4.13. This experiment was conducted in water.

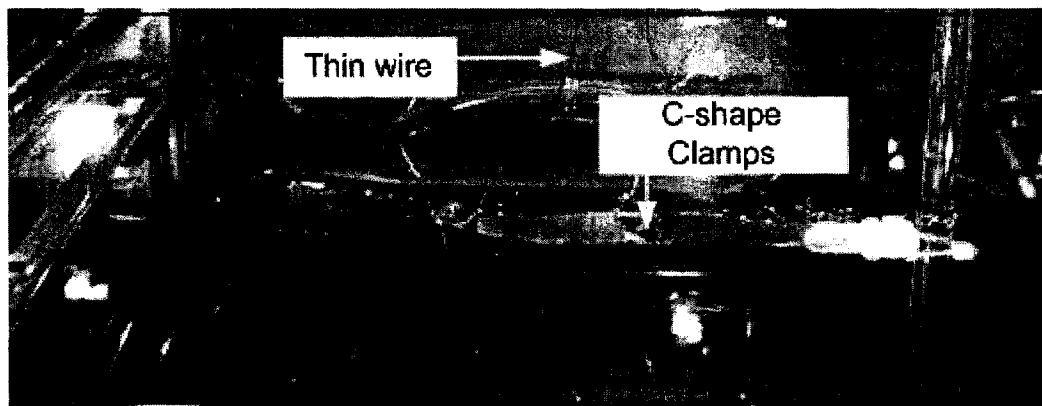


Figure 4.13 Experiment setup of Segmented ionic polymer

Input waves patterns are designed and converted to voltage signals by DA converter (dSPACE 1104). In this experiment, the input current is regulated using the Galvonostat (HA 151) instead of voltage for more direct control of bending in each segment. The control signals to the amplifier are sinusoidal waves as shown in Figure 4.14 (a).

It should be noted that the three sinusoidal signal shown in Figure 4.14 (a) has different phase to generate phase the undulatory motion compared with single segment oscillatory bending motion. An effort has been made to monitor the deflection of the segmented IPMC but the reflection in the water and thin wire connectors were some concerns that did not allow the vision system function properly. Addressing the above

issues would make the future experiment setup serves as better for motion acquisition of the segmented ionic polymer in the water.

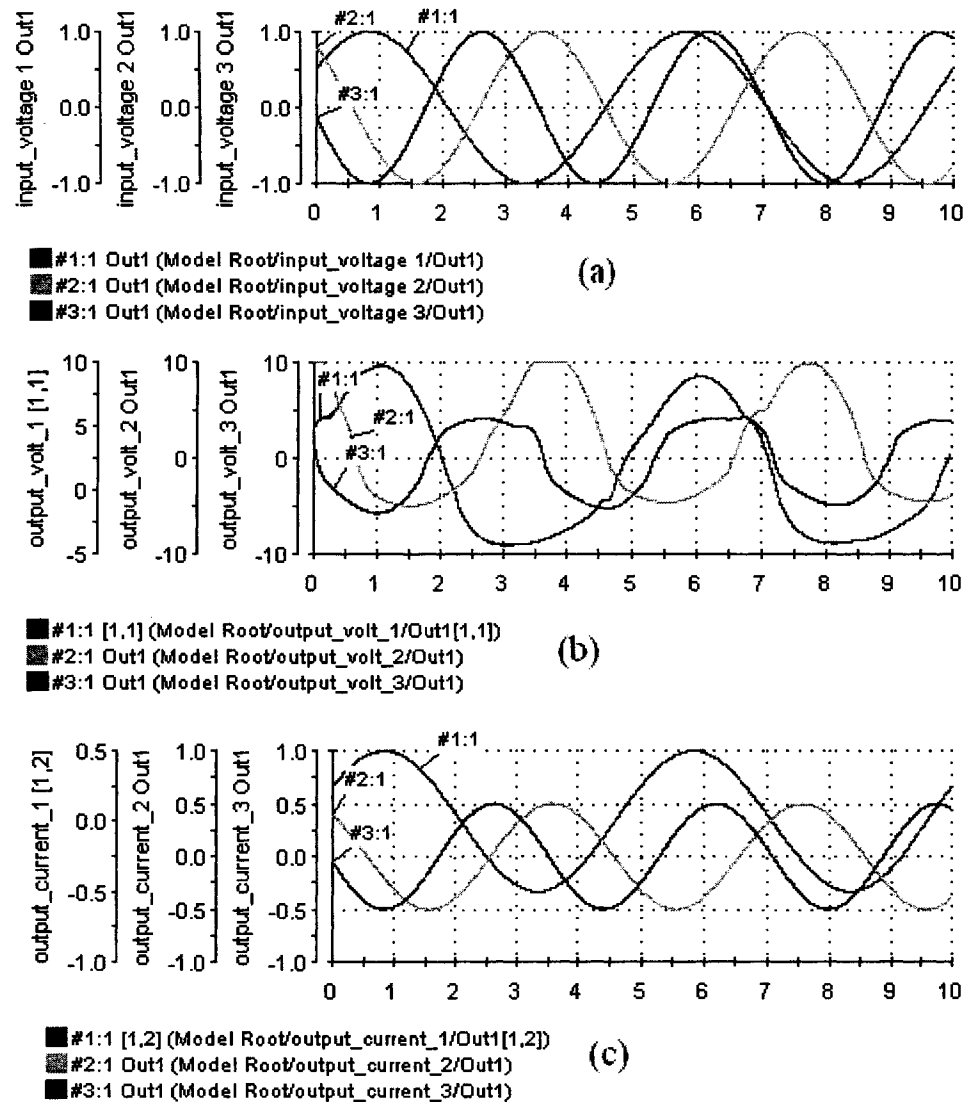


Figure 4.14 Input voltage and output response segmented ionic polymer

(a) Programmed signal (b) Out put voltage signal (c) Output current

4.2 Computer simulated results of segmented ionic polymer

A computer program has been developed to simulate the dynamics of the single and segmented ionic polymer developed in chapter 2. The state space model Equation 2.28 was simulated using Matlab. For the feasibility study of using the segmented ionic polymer strip for underwater propulsion application, the similar ionic polymer strip parameters used in [11] is used. The following table shows the simulation and material parameters used in computational study.

Table 4-2

R_1	160 Ω
R_2	800 Ω
C	1000E-5 F
Z	0.24
P	0.1
τ_2	10 s
$\tau_1(=R_1C)$	0.23 s
a (length of polymer)	0.05 m
b (width of ionic polymer)	0.01 m
E_b (modulus for Nafion)	5E7 Pa
E_p (modulus for electrode(Pt))	144E9 Pa
h_b (thickness of Nafion)	0.00028 m
h_p (thickness of electrode)	0.000002 m
ρ_b (density of Nafion)	2600 kg/m^3
ρ_p (density of electrode(Pt))	21500 kg/m^3

Simulation was performed for the step input voltage of $V = \{2 \ 1 \ -2\}^T$ for the three segment ionic polymer . Figure 5.14 and Figure 5.15 shows the input step voltage applied to each segment and simulated nodal displacement. It should be noted that Eq (2.28) is developed based on the small deflection assumption, which means that each point on the ionic polymer doesn't have any motion in axial direction.

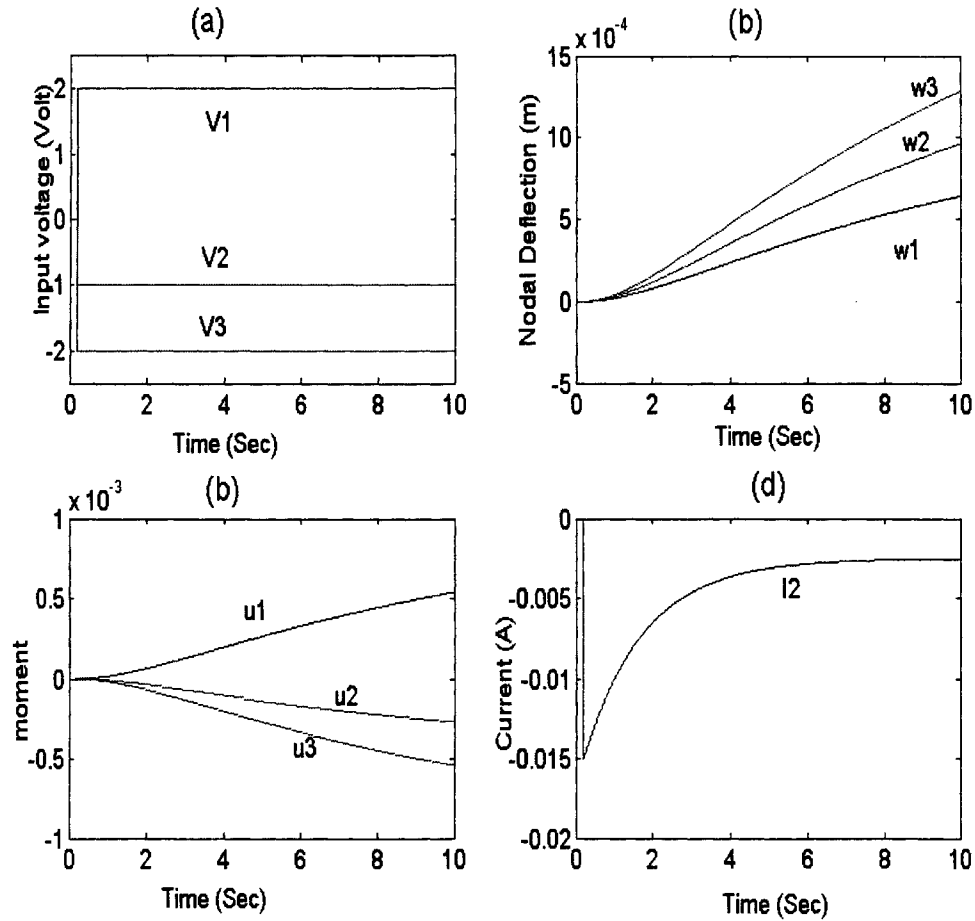


Figure 4.15 Simulated plots for 2V, 1V and -2V (n=3)

(a) Input step voltage plot, (b) Nodal displacement plots, (c) Bending moment plots for each segment, and (d) Input current plot segment 2

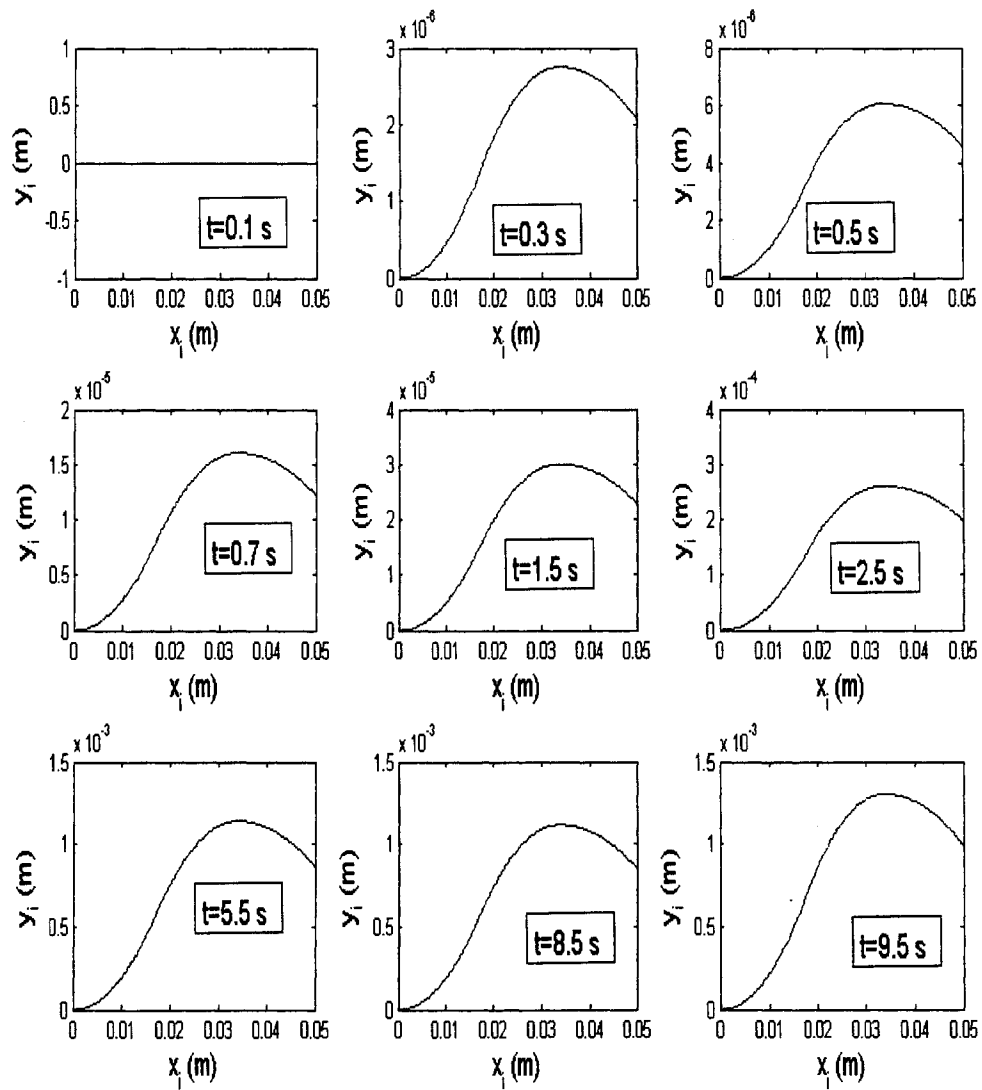


Figure 4.16 Simulated plots for 2V, 1V and -2V ($n=3$)

4.3 Experimental validation of the simulation results.

To validate the computer simulation results based on Eq (2.28), the tip motion of the ionic polymer is observed and compared with the simulation results. In this experiment

the single segment ionic polymer ($50 \times 10 \times .29 \text{ mm}$) is used and step input of 2.5V and 3V are applied. Figure 4.17 and 4.18 show the time domain tip and current responses of the ionic polymer.

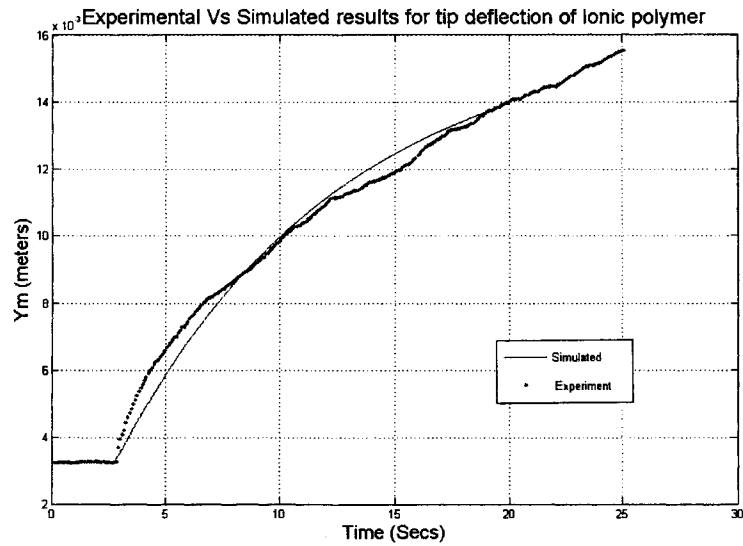


Figure 4.17 Experimental Vs Simulated tip Deflection for step input 2.5V

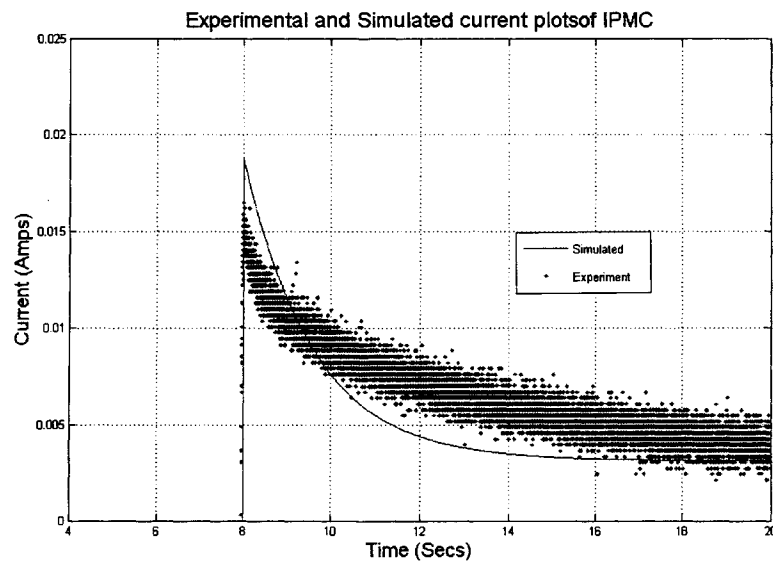


Figure 4.18 Experimental Vs Simulated current response

Figure 4.19 shows the shape response of the ionic polymer 2.5 V step input. Figure 5.19, Figure 5.20 and Figure 5.21 show the tip, current and shape responses of the 3 V step input respectively. All the output had same shape, amplitude and agreed well.

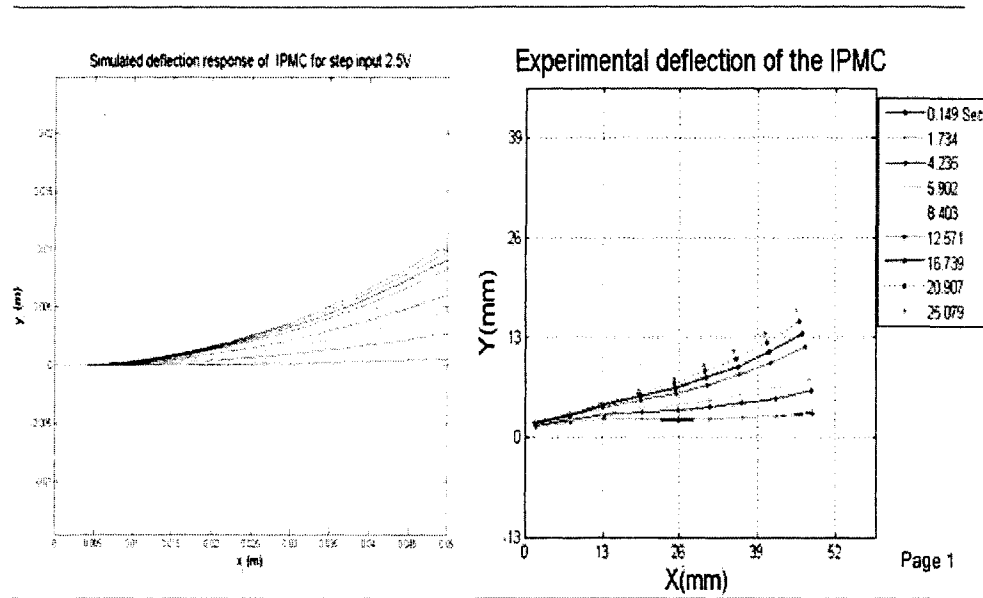


Figure 4.19 Simulated and Experimental Shape of ionic polymer for 2.5V step input

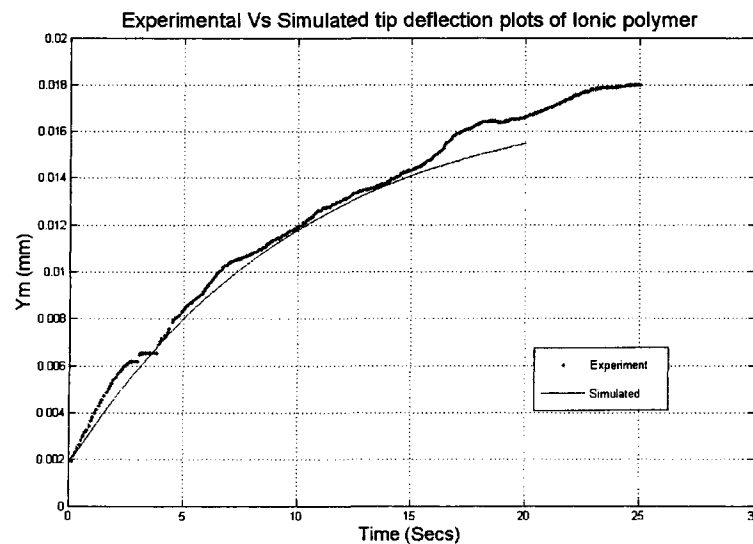


Figure 4.20 Experimental Vs Simulated tip deflection for step input 3V

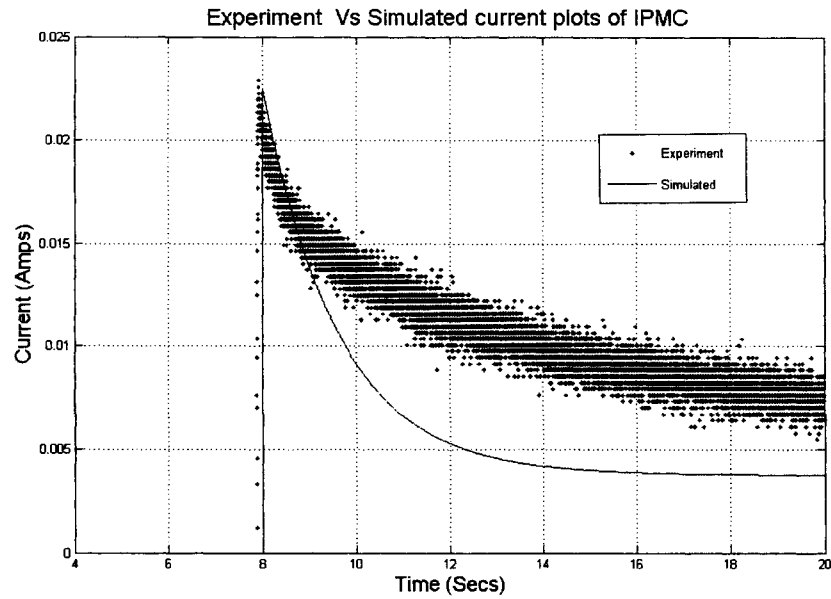


Figure 4.21 Experimental Vs Simulated current response for 3 V

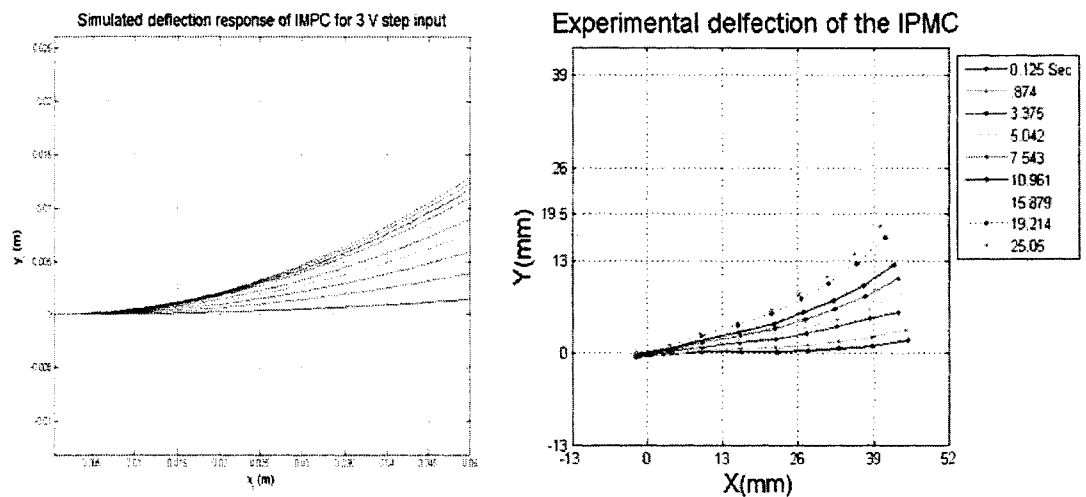


Figure 4.22 Simulated and Experimental shape of ionic polymer for 3V step input

CHAPTER 5

CONCLUSION AND FUTUREWORK

5.1 Conclusion

Ionic polymer is group of ionic EAP (Electro Active Polymer) with performances and materials characteristics that are strongly dependent on the material constituents, fabrication process and history. The performances may vary as result of ion exchange with the water in which the material is immersed. Therefore the documented performances that are mentioned in this thesis may be meaningful only to the particular samples and particular test conditions.

Accurate information about dynamic properties of the ionic polymer is important to designers who would consider the construction of mechanisms or devices using these ionic polymers. In this thesis, finite element based analytical model is proposed for single and segmented configuration. This analytical model can be applied for both single and segmented IPMC which can exhibit varying curvature along the polymer. The model is flexible enough to conveniently accommodate the relaxation behavior of ionic polymer.

Modeling of the ionic polymer involves RC circuit based electrical model and beam model based mechanical model. The actual parameters of the models can be found from experiments conducted [11]. It is expected that eventually microscopic description of the polymer may help to identify these parameters in more convincing way.

Observed deformation of the ionic polymer is digitized using a video camera and image processing algorithm. An intensity filtration and image morphing algorithm are used to acquire the deformed shape of the ionic polymer sample at sequential time interval. This increases the efficiency of deflection monitoring system when compared to the usage of Laser Vibrometer at the expense of slower rate of acquisition. Also the proposed vision system is capable of giving the tip position value for every given voltage, giving a scope for implementing the closed loop system in the future.

5.2 Recommended future work

The work done in this report is basically to understand the characteristics the ionic polymer and develop the experimental setup for performing various data acquisition and control operation. The response for various step voltages give the basic idea of dynamic properties of the ionic polymer. The proposed analytical model holds good for voltages with both high and low frequencies. However, there are several areas that need to be investigated further.

5.2.1 Large deflection model

Simulated model of the ionic polymer proposed in this thesis is validated for small deflection of the ionic polymer. In real case, the ionic polymer deflection can be large and necessary model that can handle large deflection is needed along with proper model of viscoelasticity of the polymer

5.2.2 Segmented ionic polymer

An experimental setup is developed to understand the working the segmented ionic polymer motion for different voltage. A thin wire and C type clamps are used to connect the electrodes to polymer. However, there is the need to develop suitable technique of connecting of electric wires to each segment without obstructing the motion of the polymer. This is illustrated in Figure 4.13. Further tuning of the model parameters is necessary to validate the response of the segmented ionic polymer

5.2.3 Hydrodynamic modeling

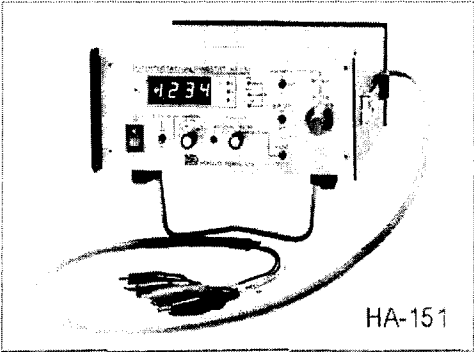
This ionic polymer finds application in an aquatic atmosphere which implies that hydrodynamic forces should be considered in the analytical model.

5.2.4 Control

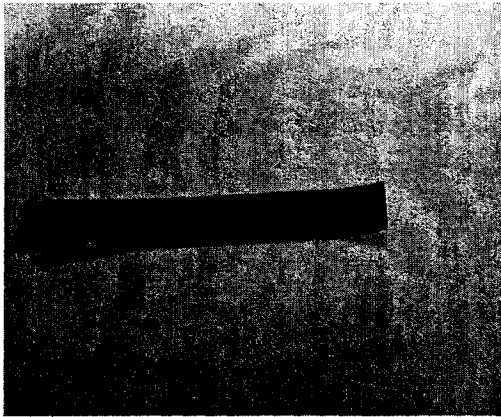
Based on the state space model developed in this thesis, the closed loop control algorithm can be derived for controlling the motion of the polymer. This can be accomplished by synchronizing the vision system along with the control signal.

APPENDIX A – EXPERIMENTAL APPARATUS

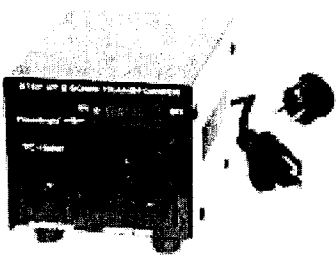
A.1 Bi - Polar Voltage amplifier

 <p>HA-151 Hakuto Denko</p>	<p>Power Requirements</p> <ul style="list-style-type: none"> - AC100V $\pm 10\%$, 50-60Hz, 100VA <p>Electrical Specifications</p> <ul style="list-style-type: none"> - Maximum Output voltage $\pm 15V$ - Maximum Output current $\pm 1A$ - Response Time 50 Micro Seconds <p>Physical</p> <ul style="list-style-type: none"> - Dimensions 220(W)x100(H)x360(D)mm - Weight 7.7 kilogram
---	---

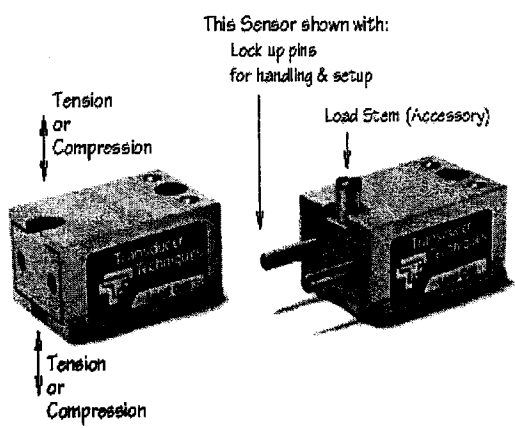
A.2 Ionic Polymer Metallic Composite Actuator

 <p>Ionic polymer</p>	<p>Specifications</p> <ul style="list-style-type: none"> - Thickness = 0.3mm - $d_{31} = -1.750 \times 10^{-7} \text{ m/V}$ - $V_{\text{max}} = 4V$ - $V_{\text{min}} = -4V$ - Polymer Type= Perfluorinate sulfonate - Young's Modulus = 1.158Gpa - Poisson's ratio = 0.487
--	--

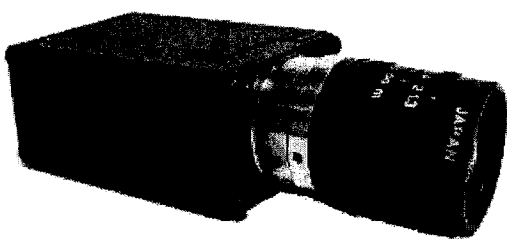
A.3 Step UP/Down Transformer

	<p>Specification</p> <p>Electrical Specifications</p> <ul style="list-style-type: none"> - Input voltage 110/200/220/240 Volt - Output voltage 110/220-240 Volt <p>Physical</p> <ul style="list-style-type: none"> - Dimensions 3.7 x 5.2 x 3.5 inches - Weight 3.52 Lbs
---	---

A.4 Load Cell

	<ul style="list-style-type: none"> - Temperature range 60 to 160 degree. - Excitation voltage 10 volts - Non repeatability 0.05 of rated output.
--	---

A.5 Camera

 <p style="text-align: center;">BASLER A602f</p>	<p>Specifications</p> <ul style="list-style-type: none"> - C-Mount, 656x491 square pixels, 100 fps, external trigger. - 1/2 inch monochrome CMOS. - Area of interest scanning with higher frame rates at lower resolutions.
---	---

A.6 dSPACE DS-1104 Controller board

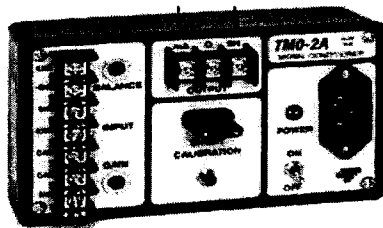


dSPACE DSP controller board

Specifications

- 8ADCs, 8 DACs
- ± 10 V input and output range
- 2 incremental encoder interfaces
- RS-232 interface.
- RS-423 interface.

A.7 Signal Conditioner



TMO 02 signal conditioner

- Type Low pass, 6 db, octave.
- Frequency is 16 Hz standard.
- Weight about 2lbs
- Dimensions 3 x 3.75 x 6.25

A.8 Rapid Prototyping Machine



Dimension SST 3-D rapid prototyping
machine

Specifications

- Fin Profile: NACA 0026
- Chord of 7 inches
- Span of 4.2 inches

APPENDIX B – MATLAB® CODE

B.1 image_cap_movie_generator.m

```
****Program to generate movie file in avi format of the captured images**  
**** following are the steps involved**  
**** Using 'GETFRAME' function making matlab movie file**  
**** converting the matlab movie file in to avi format**  
  
fprintf ( 1, '\n' );  
fprintf ( 1, 'MAKE_AVI_MOVIE\n' );  
fprintf ( 1, ' Create an AVI animation of images,\n' );  
fprintf ( 1, ' generating one frame at a time.\n' )  
  
numframes = nFrames;  
  
for i=1:numframes  
    colormap(gray);  
    real=photo(1:480,1:640,1:1,i);imagesc(real);  
    M(i)=getframe;  
end  
  
num_frames_per_second = 3;  
dur = numframes / num_frames_per_second;  
MOVIE2AVI(M, 'actual_mov', 'compression', 'None', 'fps', 3, 'quality', 75)  
  
fprintf ( 1, '\n' );  
    fprintf ( 1, 'This movie will contain %d frames.\n', numframes );  
    fprintf ( 1, 'The number of frames per second will be %d\n',  
num_frames_per_second );  
    fprintf ( 1, 'so the movie should take %d seconds to play.\n', dur );  
fprintf ( 1, '\n' );  
    fprintf ( 1, 'MAKE_AVI_MOVIE\n' );  
    fprintf ( 1, 'Normal end of execution.\n' );  
    fprintf ( 1, 'The movie file of actual_mov has been created.\n' );
```

B.2 vol_cur.m

```
***** july 10th 2005*****  
% Program for plotting the current,input voltage,output voltage response of the  
IPMC for given voltage  
% load the .map files in the folder 'Constant_voltage experiment  
% Run the program  
clear all  
clc  
  
load nexp_4volt_1amp;  
  
TITLE('plot illustrating the current,in/out volt response of IPMC');  
  
subplot(3,1,1)
```

```

plot(nexp_4volt_lamp.X.Data,nexp_4volt_lamp.Y(1).Data,'r');
TITLE('plots illustrating the current,in/out volt response of IPMC');
xlabel('Time in seconds');
ylabel(' input Voltage(volts)');
axis([0 16 -0.05 6]);
grid on
hold on

subplot(3,1,2)
plot(nexp_4volt_lamp.X.Data,nexp_4volt_lamp.Y(2).Data,'b');
xlabel('Time in seconds');
ylabel(' output Voltage(volts)');
axis([0 16 -0.05 6]);
hold on
grid on

subplot(3,1,3)
plot(nexp_4volt_lamp.X.Data,nexp_4volt_lamp.Y(3).Data,'g');
xlabel('Time in seconds');
ylabel(' current(Amps)');
axis([0 16 -0.05 .35]);
grid on

```

B.3 tip_deflection.m

```

%%this plot generates lebeles the data points in every image and calculates
%centroid
i=1
for j=1
i=1;
    maximum_intensity= imhmax(photo(1:480,1:640,1:1,j),2);
    BW = imextendedmax(maximum_intensity,65,8);
    [labeled,numObjects] = bwlabel(BW,8);
    dotdata = regionprops(labeled,'basic');
    dot_1(:, :, j)=dotdata(i).Centroid;
    dot_2(:, :, j)=dotdata(i+1).Centroid;
    dot_3(:, :, j)=dotdata(i+2).Centroid;
    dot_4(:, :, j)=dotdata(i+3).Centroid;
    dot_5(:, :, j)=dotdata(i+4).Centroid;
    dot_6(:, :, j)=dotdata(i+5).Centroid;
    dot_7(:, :, j)=dotdata(i+6).Centroid;
    dot_8(:, :, j)=dotdata(i+7).Centroid;
    dot_9(:, :, j)=dotdata(i+8).Centroid;
    dot_10(:, :, j)=dotdata(i+9).Centroid;
    dot_11(:, :, j)=dotdata(i+10).Centroid;
    dot_12(:, :, j)=dotdata(i+11).Centroid;
    dot_13(:, :, j)=dotdata(i+12).Centroid;
    dot_14(:, :, j)=dotdata(i+13).Centroid;
end
for j=1
    x_1(j,1)=dot_1(1,1,j);
    y_1(j,1)=dot_1(1,2,j);
    x_2(j,1)=dot_2(1,1,j);
    y_2(j,1)=dot_2(1,2,j);
    x_3(j,1)=dot_3(1,1,j);
    y_3(j,1)=dot_3(1,2,j);
    x_4(j,1)=dot_4(1,1,j);
    y_4(j,1)=dot_4(1,2,j);
    x_5(j,1)=dot_5(1,1,j);
    y_5(j,1)=dot_5(1,2,j);
    x_6(j,1)=dot_6(1,1,j);
    y_6(j,1)=dot_6(1,2,j);

```

```

x_7(j,1)=dot_7(1,1,j);
y_7(j,1)=dot_7(1,2,j);
x_8(j,1)=dot_8(1,1,j);
y_8(j,1)=dot_8(1,2,j);
x_9(j,1)=dot_9(1,1,j);
y_9(j,1)=dot_9(1,2,j);
x_10(j,1)=dot_10(1,1,j);
y_10(j,1)=dot_10(1,2,j);
x_11(j,1)=dot_11(1,1,j);
y_11(j,1)=dot_11(1,2,j);
x_12(j,1)=dot_12(1,1,j);
y_12(j,1)=dot_12(1,2,j);
x_13(j,1)=dot_13(1,1,j);
y_13(j,1)=dot_13(1,2,j);
x_14(j,1)=dot_14(1,1,j);
y_14(j,1)=dot_14(1,2,j);
end

```

B.4 Act_4volt.m

```

%****july 19th****
%****program to plot the Deflection of IPMC****
clear all
clc
load 4_volts_deflection;

x1=[x_4(1) x_5(1) x_6(1) x_7(1) x_8(1) x_9(1) x_10(1) x_11(1) x_12(1)
x_13(1)];
y1=[y_4(1) y_5(1) y_6(1) y_7(1) y_8(1) y_9(1) y_10(1) y_11(1) y_12(1)
y_13(1)] ;
plot(x1,y1,'b.-')
hold on
x2=[x_4(10) x_5(10) x_6(10) x_7(10) x_8(10) x_9(10) x_10(10) x_11(10)
x_12(10) x_13(10)];
y2=[y_4(10) y_5(10) y_6(10) y_7(10) y_8(10) y_9(10) y_10(10) y_11(10)
y_12(10) y_13(10)] ;
plot(x2,y2,'g.-')
hold on
x3=[x_4(20) x_5(20) x_6(20) x_7(20) x_8(20) x_9(20) x_10(20) x_11(20)
x_12(20) x_13(20)];
y3=[y_4(20) y_5(20) y_6(20) y_7(20) y_8(20) y_9(20) y_10(20) y_11(20)
y_12(20) y_13(20)] ;
plot(x3,y3,'r.-')
hold on
x4=[x_4(30) x_5(30) x_6(30) x_7(30) x_8(30) x_9(30) x_10(30) x_11(30)
x_12(30) ];
y4=[y_4(30) y_5(30) y_6(30) y_7(30) y_8(30) y_9(30) y_10(30) y_11(30)
y_12(30) 1];
plot(x4,y4,'y.-')
hold on
x5=[x_4(40) x_5(40) x_6(40) x_7(40) x_8(40) x_9(40) x_10(40) x_11(40)
x_12(40) ];
y5=[y_4(40) y_5(40) y_6(40) y_7(40) y_8(40) y_9(40) y_10(40) y_11(40)
y_12(40) 1];
plot(x5,y5,'c.-')
hold on
x6=[x_4(45) x_5(45) x_6(45) x_7(45) x_8(45) x_9(45) x_10(45) x_11(45) ];
y6=[y_4(45) y_5(45) y_6(45) y_7(45) y_8(45) y_9(45) y_10(45) y_11(45) 1];
plot(x6,y6,'k.-')

```

```

axis([160 650 160 650]);
grid on
TITLE('plot illustrating the Deflection of the IPMC');
xlabel('milli meter ');
ylabel('milli meter');
nd('2.5517
Sec','2.969','3.385','4.2188','5.0524','5.886','6.719','7.553','8.387','9.220',
'10.054','12.555','16.722','19.223','23.391','Location','NorthEastOutside');
axis ij;
% set(gca,'YTick',[40 60 80 100 120 140 160 180 200 220 240 ]);
% set(gca,'YTickLabel','0|2.6|5.2|7.8|10.4|13|15.6|18.2|20.8|23.4|26');
% set(gca,'Xtick',[100 200 300 400 500 600]);
% set(gca,'XTickLabel','0|13|26|39|52|65');

```

B.5 IPMC_tip_deflection.m

```

v%*****july 27th 2005
%*****program excutes the plot of tip deflection of ipmc
% clear all
% clc
% load actual_tip_deflection

figure(1)
plot3(x_tip,y_tip,tip_time,'r');
axis([400 480 0 250 0 25 ]);
grid on
TITLE('plot illustrating the tip Deflection of the IPMC Vs time ');
xlabel('x-axis in milli meter ');
ylabel('y-axis in milli meter');
zlabel('time');
set(gca,'YTick',[20 70 120 170 220 ]);
set(gca,'YTickLabel','0|6.5|13|19.5|26');
set(gca,'Xtick',[400 430 450 470]);
set(gca,'XTickLabel','39|42.8|45.5|48.1');

figure(2)
subplot(2,2,1:2)
plot(x_tip,y_tip,'k.-');
axis([420 480 0 250]);
grid on
axis ij;
TITLE('X-axis Vs Y-axis ');
xlabel('x-axis in milli meter ');
ylabel('y axis in milli meter');
set(gca,'Xtick',[430 450 470]);
set(gca,'XTickLabel','42.8|45.5|48.1');
set(gca,'YTick',[20 40 60 80 100 120 140 160 180 200 220 ]);
set(gca,'YTickLabel','0|2.6|5.2|7.8|10.4|13|15.6|18.2|20.8|23.4|26');
hold on
subplot(2,2,3)
plot(time,x_tip,'b.-')
grid on
TITLE('X-axis Vs time ');
xlabel('time (Seconds) ');
ylabel(' X-axis in milli meter');
set(gca,'Ytick',[430 450 470]);
set(gca,'YTickLabel','42.8|45.5|48.1');
hold on
subplot(2,2,4)
plot(time,y_tip,'b.-')
set(gca,'YTick',[20 70 120 170 220 ]);
set(gca,'YTickLabel','0|6.5|13|19.5|26');

```



```

grid on
TITLE('Y-axis Vs time ');
xlabel('time (Seconds) ');
ylabel(' Y-axis in milli meter');

```

B.6 main.m

```

%%%%%%%%%%%%%%%%%%%%%%%%%%%%%%%%%%%%%%%%%%%%%%%%%%%%%%%%%%%%%%%%%%%%%%%%
% Simulation program for IPMC for single and multiple segments
% %%%%%%%%%%%%%%%%%%%%%%%%%%%%%%%%%%%%%%%%%%%%%%%%%%%%%%%%%%%%%%%%%%%%%%%%%
global An Bn Cn Dn
global a; % length of IPMC
global a_0 a_1 b_0 b_1; % u/V
global n; %number of elements used for simulation
global Li;
global EIi;
global rhoi;
global t_plt
%
n=3; %Define number of elements
t_plt=[0.1 0.3 0.5 0.7 1.5 2.5 5.5 8.5 9.5 ]; %For beam plot by plt_beam
% For choosing nodal displ selection for sink in sim_1 simulink prog
for i=1:n
    out_selector(i)=2*i-1;
end
i_selector=[1]; %for plot of current I in sim_1
% define system parameters
% RC circuit and relaxation model
R1=160;
R2=700;
C=1000e-7;
K1=4.87e-4/C; %m/volt
K2=1.07e-3/C; %m/volt
tau2=10;
tau1=R1*C;
% IPMC
a=0.05;%Total length of IPMC (m)
Li=a/n;% element length
bb=0.01;%Width of the IPMC (m)
bp=0.01;%Width of platinum electrode (m)
hb=0.0002818;%Height of the Nafion polymer (m)
hp=0.000002; %Thickness of Platinum coating (m)
Eb=5*10^7; %Modulus of Elasticity for Nafion (Pa)
Ep=144*10^9; %Modulus of Elasticity of the piezoelectric film (Pa)

%Assume that mass is uniformly distributed
rhob=2600; %density of Nafion (kg/m^3)
rhop=21500; %density of electrode (kg/m^3)

%Preliminary calculations
Li=a/n; %length of each element (m)
rhoi=rhob*bb*hb+2*rhop*bp*hp; %linear mass density of each element
%Area moment of inertia calculations. Use an equivalent beam
Ab=hb*bb; %area of the beam section
bpe=(Ep*bp)/Eb;%equivalent width of a similar section made of beam material
Ape=bpe*hp; %equivalent area of a similar section
made of beam material
na=0; %neutral axis location (symmetry)
Ii=((bb*hb^3)/12)+2*((bpe*hp^3)/12)+2*(Ape*((0.5*hp+0.5*hb)-na)^2);
EIi=Eb*Ii;
% calculate M_b/V model parameters
b_1=0;

```

```

b_0=K1*C/(tau1*tau2)
a_1=(tau1+tau2)/(tau1*tau2);
a_0=1/(tau1*tau2);
%strain coefficient of IPMC
% size for mass matrix before reduction
var_num=2*(n+1);
%define the rank of each matrix
sum_Mexi=zeros(var_num,var_num);
sum_Kexi=zeros(var_num,var_num);
sum_Fexi=zeros(var_num,n);
%Expand element matrix for total beam
for i=1:n
    sum_Mexi=sum_Mexi+mexi(i);
end;
%the total mass matrix
M=sum_Mexi;
%generate the stiffness matrices
for i=1:n
    sum_Kexi=sum_Kexi+kexi(i);
end;
% total stiffness matrix
K=sum_Kexi;
%generate force matrix
for i=1:n
    sum_Fexi=sum_Fexi+fexi(i);
end
F=sum_Fexi;
%reduced the dynamical model based on the displacement boundary condition
reduced_M=M(3:var_num,3:var_num);
reduced_K=K(3:var_num,3:var_num);
reduced_F=F(3:var_num,:);
% inverse of mass matrix
iM=inv(reduced_M);

%*****
% state space model:
% *****
% make vectors for a_0 a_1 b_0 b_1
for i=1:n
    a_0n(i)=a_0;
    a_1n(i)=a_1;
    b_0n(i)=b_0;
    b_1n(i)=b_1;
end
Be=reduced_F;
Bv=[zeros(n,n);eye(n)];
Bu=[diag(b_0n) diag(b_1n)];
Az=[zeros(n,n) eye(n);-diag(a_0n) -diag(a_1n)];
An=[zeros(2*n),eye(2*n) zeros(2*n); ...
    -iM*reduced_K,zeros(2*n),iM*Be*Bu; ...
    zeros(2*n), zeros(2*n), Az];
Bn=[zeros(2*n,n);zeros(2*n,n);Bv];
Cn=[eye(2*n) zeros(2*n,2*n) zeros(2*n,2*n);...
    zeros(2*n,2*n) zeros(2*n,2*n) eye(2*n)];
Dn=[zeros(4*n,n)];

```

B.7 fexi.m

```

function Fexi=fexi(i)
%This matrix generates mass matrix of an element i and expands it.

global n;

```

```

global ui;
global Li;
global EIi;
global rhoi;
global c;
global u;

global ui;
global iM;
global C;
global K;
global D;

%Define matrix size
var_num=2*(n+1);

% Initialize the matrices
Fvi=[0;-1;0;1];
Fexi=zeros(var_num,n);
Fexi(2*i-1:2*i+2,i)=Fvi;

```

B.8 mexi.m

```

function Mexi=mexi(i)
%This matrix generates mass matrix of an element i and expands it.
global n;
global ui;
global Li;
global EIi;
global rhoi;
global c;
global u;

global ui;
global iM;
global C;
global K;
global D;

%Define matrix size
var_num=2*(n+1);

% Initialize the matrices
Mvi=zeros(4,4);
Mexi=zeros(var_num,var_num);

rho=rhoi;
X_i=Li*(i-1);
%C(Mvi,optimized);
t1 = rho*Li; t2 = Li*Li; t3 = rho*t2; t5 = rho*t2*Li;
if(i~=n)
Mvi(1,1) = 13.0/35.0*t1;
Mvi(1,2) = 11.0/210.0*t3;
Mvi(1,3) = 9.0/70.0*t1;
Mvi(1,4) = -13.0/420.0*t3;
Mvi(2,1) = 11.0/210.0*t3;
Mvi(2,2) = t5/105;
Mvi(2,3) = 13.0/420.0*t3;
Mvi(2,4) = -t5/140;
Mvi(3,1) = 9.0/70.0*t1;
Mvi(3,2) = 13.0/420.0*t3;

```

```

        Mvi(3,3) = 13.0/35.0*t1;
        Mvi(3,4) = -11.0/210.0*t3;
        Mvi(4,1) = -13.0/420.0*t3;
        Mvi(4,2) = -t5/140;
        Mvi(4,3) = -11.0/210.0*t3;
        Mvi(4,4) = t5/105;
    else
        Mvi(1,1) = 13.0/35.0*t1;
        Mvi(1,2) = 11.0/210.0*t3;
        Mvi(1,3) = 9.0/70.0*t1;
        Mvi(1,4) = -13.0/420.0*t3;
        Mvi(2,1) = 11.0/210.0*t3;
        Mvi(2,2) = t5/105;
        Mvi(2,3) = 13.0/420.0*t3;
        Mvi(2,4) = -t5/140;
        Mvi(3,1) = 9.0/70.0*t1;
        Mvi(3,2) = 13.0/420.0*t3;
        Mvi(3,3) = 13.0/35.0*t1;
        Mvi(3,4) = -11.0/210.0*t3;
        Mvi(4,1) = -13.0/420.0*t3;
        Mvi(4,2) = -t5/140;
        Mvi(4,3) = -11.0/210.0*t3;
        Mvi(4,4) = t5/105;
    end;
%Expand mass matrix in terms of the global coordinates
Mexi(2*i-1:2*i+2,2*i-1:2*i+2)=Mvi;

```

B.9 kexi.m

```

function Kexi=kexi(i)
%This matrix generates stiffness matrix of an element i and expands it.

global n;
global ui;
global Li;
global EIi;
global rhoi;
global c;
global u;

global ui;
global iM;
global C;
global K;
global D;

%Define matrix size
var_num=2*(n+1);
EIvi=EIi;

% Initialize the matrices
Kvi=zeros(4,4);
Kexi=zeros(var_num,var_num);

    X_i=Li*(i-1);

    %C(Kvi,optimized);
    t1 = Li*Li;
    t4 = EIvi/t1/Li;
    t6 = EIvi/t1;

```

```

t8 = EIvi/Li;
Kvi(1,1) = 12.0*t4;      Kvi(1,2) = 6.0*t6;
Kvi(1,3) = -12.0*t4;     Kvi(1,4) = 6.0*t6;
Kvi(2,1) = 6.0*t6;      Kvi(2,2) = 4.0*t8;
Kvi(2,3) = -6.0*t6;     Kvi(2,4) = 2.0*t8;
Kvi(3,1) = -12.0*t4;    Kvi(3,2) = -6.0*t6;
Kvi(3,3) = 12.0*t4;     Kvi(3,4) = -6.0*t6;
Kvi(4,1) = 6.0*t6;      Kvi(4,2) = 2.0*t8;
Kvi(4,3) = -6.0*t6;     Kvi(4,4) = 4.0*t8;

%Expand stiffness matrix in terms of the global coordinates
Kexi(2*i-1:2*i+2,2*i-1:2*i+2)=Kvi;

```

B.10 plt_beam.m

```

%This generates the deflection shapes of the segmented IPMC
global t_plt
% number of plots
dum=size(t_plt);
ip=dum(1,2);
iw=size(w_phi);
n_data=iw(1,1);
%plot for each ip
for j=1:ip
    for ii=1:n_data
        del=t(ii)-t_plt(j);
        if(abs(del)<1e-8)
            t(ii)
            out=w_phi(ii,:);
%assign nodal coordinate for each element i
            node(1,1)=0;
            node(1,2)=0;
            node(1,3)=out(1);
            node(1,4)=out(2);
            if n >= 2
                for i=2:n
                    node(i,1)=out(2*(i-1)-1);
                    node(i,2)=out(2*(i-1));
                    node(i,3)=out(2*(i-1)+1);
                    node(i,4)=out(2*(i-1)+2);
                end
            end
        end
    end
% get the shape of the IPMC
    delx=Li/50;
    k=1;
    sumx=0;

    for i=1:n
        node_vector=node(i,:);
        node_x=0;
        for jj=1:50
            w_all(j,k)=get_w(node_vector,node_x);
            node_x=node_x+delx;
            sumx=sumx+delx;
            x_all(k)=sumx;
            k=k+1;
        end
    end
end
end
end

```

```

end
end
for i=1:ip
    subplot(3,3,i)
    plot(x_all,w_all(i,:));
    xlabel('x_i (m)','FontSize',13)
    ylabel('y_i (m)','FontSize',13)
end

```

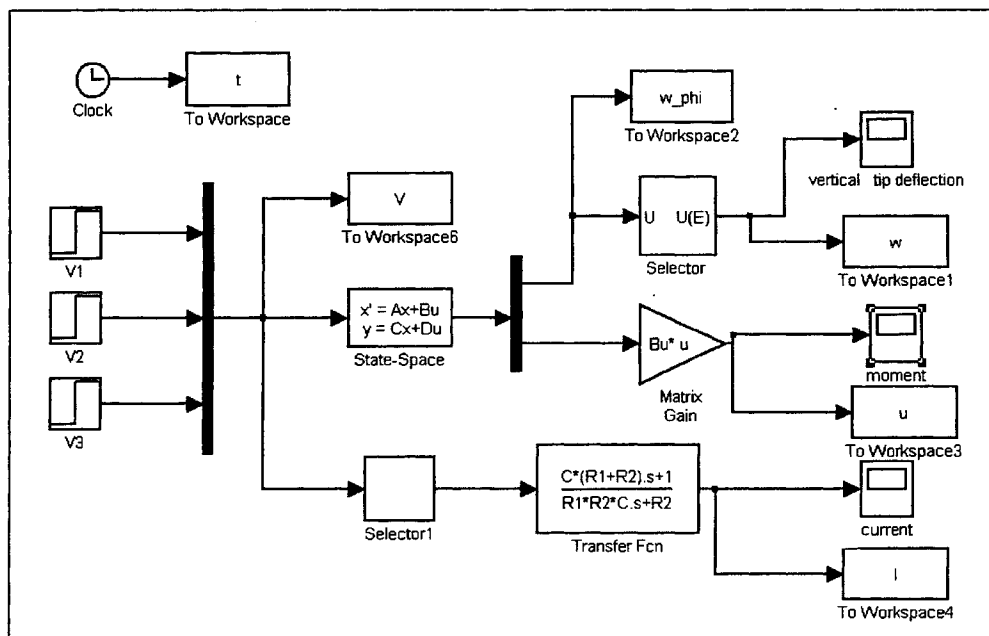
B.11 plt.-misc

```

% plots the input and electric output
subplot(2,2,1)
plot(t,V(:,1),t,V(:,2),t,V(:,3))
subplot(2,2,2)
plot(t,w(:,1),t,w(:,2),t,w(:,3))
subplot(2,2,3)
plot(t,u(:,1),t,u(:,2),t,u(:,3))
subplot(2,2,4)
plot(t,I)
y=(C*x'+D*u)';

```

B.12 sim_1.m



BIBLIOGRAPHY

- [1] Shahinpoor, M., Bar-Cohen, Y., Simpson, J., and Smith, J., "Ionic Polymer-Metal Composites (IPMCs) as Biomimetic Sensors, Actuators and Artificial Muscles - a Review," *Smart Materials and Structures*, Vol. 7, No. 6, pp. R15 -R30, 1998.
- [2] Kanno, R., Kurata, A., Hattori, M., Tadokoro, S., Takamori, T., and Oguro, K., 1994, "Characteristic and Modeling of ICPF Actuator," in: proceedings of the japan-USA *Symposium on Flexible Automation*, Vol. 2, pp. 691-698.
- [3] Kanno, R., Tadokoro, S., Takamori, T., and Hattori, M., 1996, "Linear Approximate Dynamic Model of ICPF Actuator," in: *Proceedings of the IEEE International Conference on Robotics and Automation*, pp. 219-225.
- [4] Newbury, K. and Leo, D., "Electromechanical Modeling and Characterization of Ionic Polymer Benders," to appear in *Journal of Intelligent Material Systems and Structures*, 2002.
- [5] Nemat-Nasser, S. and Li, J., "Electromechanical Response of Ionic Polymer-Metal Composites," *Journal of Applied Physics*, Vol. 87, pp. 3321-3331, 2000.
- [6] Tadokoro, S., Yamagami, S., Takamori, T., and Oguro, K., 2000, "Modeling of Nafion-Pt Composite Actuators (ICPF) by Ionic Motion," in: *Proceedings of the SPIE*, Vol. 3987, pp. 92-102.
- [7] De Gennes, P., Okumura, K., Shahinpoor, M., and Kim, K., "Mechano- electric effects in ionic gels," *EUROPHYSICS LETTERS*, Vol. 40, No. 4, pp. 513-518, 2000.
- [8] Ogura, K., Asaka, K., Fujiwara, Nonishi K., Sewa, S., "Polymer electrolyte actuator driven by low voltage," *Materials Research Society Symposium - Proceedings*, v 600, 2000, p 229-235
- [9] Nemat-Nasser, S., "Micro-mechanics of Actuation of Ionic Polymer-metal Composites (IPMCs)," to appear in *Journal of Applied Physics*, 2002
- [10] Farinholt, K. and Leo, D. 2002 . "Modeling of Electromechanical Charge Sensing in Ionic Polymer Transducers ," to appear in *Mechanics of Materials*.
- [11] X.Bao, Y.Bar-Cohen, S-S Lih, "Measurements and Macro Models of Ionomeric Polymer-Metal Composites (IPMC)," *Proceedings of the SPIE Smart Structures and Materials Symposium, EAPAD Conference ,San Diego ,CA*, March 18-21, 2002

- [12] Yim, W., Singh, S.N., Trabia, M., Drysdale, W., "Adaptive Control of projectile fin Angle Using Piezoelectric Beam Actuator," *Proceedings of the SPIE smart Structures and Materials Symposium*, San Diego, CA, March, 2004
- [13] Bar-Cohen, Y., Sherrit, S., and Lih, S., 2001a, "Characterization of the Electromechanical Properties of EAP materials," in: *Proceedings of the SPIE*, Vol. 4329, pp. 319-327.
- [14] Mojarad, M. and Shahinpoor, M., 1997a, "Ion-exchange-metal composite artificial muscle actuator load characterization and modeling," in: *Proceedings of the SPIE*, Vol. 3040, pp. 294-301.
- [15] Shahinpoor, M., "Micro-Electro-Mechanics of Ionic Polymeric Gels as Electrically Controllable Artificial Muscles," *Journal of Intelligent Material Systems and Structures*, Vol. 6, No. 3, pp. 307-314, 1995.
- [16] Shahinpoor, M., Mojarad, M., and Salehpour, K., 1997, "Electrically induced large amplitude vibration and resonance characteristics of ionic polymeric membrane-metal composites artificial muscles," in: *Proceedings of the SPIE*, Vol. 3041, pp. 829-838.
- [17] K.Ogawa, Y.Nakabo, T.Mukai, K.Asaka and N. Ohnishi "A snake –like swimming artificial muscle ," *The 2nd conference on Artificial Muscles Osaka*, 2004
- [18] K.Ogawa, Y.Nakabo, T.Mukai, K.Asaka and N. Ohnishi "A multi DOF robot manipulator with a patterned artificial muscle," *The 2nd conference on Artificial Muscles Osaka*, 2004.
- [19] Asaka, A, Oguro, K., Nishimura, Misuhata, M., Takeneka, H., "Bending of Polyelectrolyte Membrane- Platinum Composites by Electric Stimuli, I. Response Characteristics to Various Wave Forms," *Polymer Jopurnal*, 27, 1995, (436-440)
- [20] Bhattacharya, K, Li, J., and Xiao, J., "Electromechanical Models for Optimal Design and Effective behavior of Electroactive Polymers," in *Electroactive Polymer (EAP) Actuators as Artificial Muscles*, Bellingham, Washington, SPIE, 2001
- [21] De Gennes, P.G., Okumura, K., Shahinpoor, M., Kim, K. J., "Mechanoelectric Effects in Ionic Gels," *Europhysics Letters*, 50(4), 2000, (513-518).
- [22] K.Mallavarupu, K.Newbury, and D. Leo, "Feedback control of the bending response of the ionic polymer-metal composite actuators," *Proceedings of SPIE Symposium on smart Structures and Materials*, vol.4329, pp.301-310 March 2001.
- [23] K.Mallavarupu, , Feedback control of ionic polymer actuators, Masters Thesis, Virginia Polytechnic Institute and State University , July 2001

VITA

Graduate College
University of Nevada, Las Vegas

Prashanth Reddy Duvvuru Kamakshi

Local Address:

969 E Flamingo Rd
Apartment # 135
Las Vegas, Nevada 89119

Permanent Address:

S/o D. Subrahmanyam
BHEL MIG-1818 R.C.Puram
HYDERABAD., Andhra Pradesh
India - 502032

Degree:

Bachelor of Science, Mechanical Engineering, 2003
Madras University , India

Thesis Title:

Dynamic Modeling and Experimental verification of IPMC

Thesis Examination Committee:

Chairperson, Dr. Woosoon Yim, Ph. D.
Committee Member B. Trabia, Ph. D.
Committee Member, Dr. Ajit Roy, Ph. D.
Graduate Faculty Representative, Dr. Sahajendra Singh, Ph. D.